



Field survey of the 30 October 2020 Samos (Aegean Sea) tsunami in the Greek islands

Nikos Kalligeris¹ · Vassilios Skanavis² · Marinos Charalampakis¹ · Nikolaos S. Melis¹ · Evangelos Voukouvalas³ · Alessandro Annunziato⁴ · Costas E. Synolakis²

Received: 30 April 2021 / Accepted: 11 October 2021 / Published online: 23 October 2021
© The Author(s), under exclusive licence to Springer Nature B.V. 2021

Abstract

On October 30th, 2020, a magnitude 7.0 earthquake offshore off the northern coast of Samos, Greece, generated a tsunami that impacted the nearshore Greek islands and the Aegean coastline of Turkey. Here, we describe detailed results from several post-event field surveys, and report first wave arrival timing and polarity information as well as tsunami height/runup measurements, from five islands. In Chios, wave runup reached 1.38 m, in Samos ~3 m, in Fourni 1.57 m, in Thimena 1.46 m, and in Ikaria 1.18 m. This event marks two milestones. One, the General Secretariat for Civil Protection of Greece, disseminated a message through Greece's 1–1-2 Emergency Communications Service to all cell phones in the eastern Aegean geographical region, warning recipients to stay away from coastal areas. According to eyewitnesses, the message was received ~3–5 min prior to the second and largest flood in Vathi, as the first flood had not sufficiently alarmed the local authorities to evacuate residents. Two, we were able to infer complete tsunami hydrographs from measurements for the first two floods in Vathi, which suggests that the water level rose to about one meter overland flow depth in one minute.

Keywords October 2020 · Tsunami · Samos earthquake · Aegean · Field survey · Coastal impact

1 Introduction

On October 30th, 2020, at 11:51:27 UTC a magnitude 7.0 (USGS) earthquake was triggered in the Aegean Sea ~10 km offshore off the northern coast of Samos (Fig. 1) generating a tsunami that impacted the nearshore Greek islands and the Aegean coastline of Turkey. In the Greek islands, the 30 October 2020 Samos (Aegean Sea) tsunami mainly impacted the low-topography areas (below 2 m elevation) along the waterfront of Vathi,

✉ Nikos Kalligeris
nkalligeris@noa.gr

Extended author information available on the last page of the article

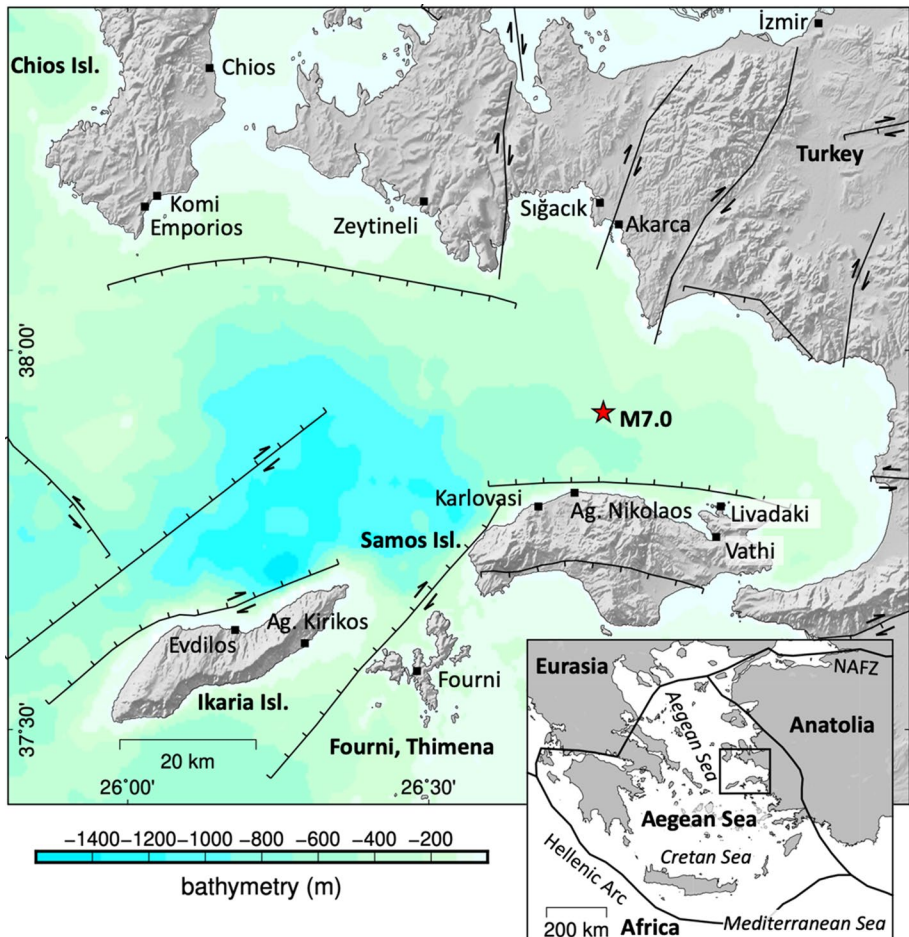


Fig. 1 Active faults according to the GEM database (Styron and Pagani 2020) and places of interest around the epicentre (red star; source: USGS) of the 30 October 2020 Samos (Aegean Sea) earthquake. The coloured background shows the GEBCO bathymetric relief (GEBCO 2020). The inset figure shows the tectonic plates and plate boundaries of the broader region (Bird 2003)

Samos, and caused minor damages in other ports and harbours in the wider region. There were no casualties from the tsunami in Greece (Triantafyllou et al. 2021), while one person's life was lost in Turkey (Aksoy 2021). Along the Aegean Turkish coast, damage from the tsunami was more extensive, with runup values as high as 3.8 m being measured in Akarca and inundation distance reaching ~760 m in Zeytineli (Dogan et al. 2021). A maximum runup of 5.3 ± 0.3 m was inferred for the town of Sigacık through satellite and topographic maps (Aksoy 2021). The earthquake shaking caused widespread damage to buildings, particularly in the Turkish city of Izmir where ~4% of the buildings sustained damage and 115 people lost their lives (Erdik et al. 2020).

The Samos (Aegean Sea) earthquake ruptured the cross-border region of the eastern Aegean microplate and western Anatolia (Fig. 1). The tectonic regime of the area is highly complex, and it is deforming due to both extensive and transtensive shear

(Tur et al. 2015; Kiratzi et al. 2020). At the plate boundary, England et al. (2015) have argued that most of the relative motion is aseismic, hence the modern record of seismicity provides little or no information about the faults that are likely to generate such earthquakes. Active faulting patterns change gradually from transtensional in the north to extensional in the south, as the distance from the North Anatolian Fault Zone (NAFZ) and its splays increases (Chatzipetros et al. 2013). The Samos earthquake is attributed to north–south extensional stress along a moderately dipping normal east–west striking fault north of Samos, as a result of the upper crust being pulled apart due to slab rollback, where the African plate is subducting northwards below the Aegean Sea and Eurasia, while the slab is sinking by gravitational forces, causing it to retreat southwards (Meng et al. 2021). A 40 km \times 15 km fault rupture area located offshore Samos with an average co-seismic slip of 1.7 m and a moderate dip-angle (37°) have been suggested by the source-inversion model of Ganas et al. (2021) that is based on Global Navigation Satellite System (GNSS) and Interferometric Synthetic Aperture Radar (InSAR) data. Lentas et al. (2021), using kinematic slip inversion, suggested a non-uniform bilateral rupture of 2.5 m maximum slip on a fault area of 60 km \times 20 km, with dip angle 34° and the main rupture propagating to the west.

The earthquake occurrence prompted the Tsunami Service Providers (TSPs) operating in the eastern Mediterranean in the framework of the North-Eastern Atlantic, Mediterranean and connected seas Tsunami Warning System (NEAMTWS) of IOC/UNESCO, namely CAT-INGV-TSP, HLNTWC-NOA-TSP and KOERI-TSP to issue tsunami warning messages. The initial tsunami warning messages that set the near-field coastal areas (distance < 100 km from the earthquake epicentre) in *Watch* threat level were all issued within 12 min from the earthquake. While reports of tsunami sightings had already circulated in social and news media within the first hour after the earthquake, the official confirmation of tsunami generation came through tsunami records at the nearest tide gauges in the islands of Syros, Lesbos and Kos (available through the Sea Level Monitoring Facility website of IOC/UNESCO, <https://www.ioc-sealevelmonitoring.org>), which were used by TSPs to issue *Watch* Ongoing tsunami warning messages (Dogan et al. 2020). The tsunami signature remained prominent in tide gauge records in the Aegean and Cretan Seas for several hours after first wave arrival (Dogan et al. 2020).

Following the broadcast of the initial tsunami warning message by HLNTWC-NOA-TSP, the Hellenic Hydrographic Service issued a NAVTEX (NAVigational TELeX) message for tsunami waves in the Aegean Sea based on the area of responsibility of the Greek Navy (Tuncag et al. 2020). Additionally, the General Secretariat for Civil Protection of Greece disseminated a message through Greece's 1–1-2 Emergency Communications Service to all cell phones in the eastern Aegean geographical area, warning recipients to stay away from coastal areas. To the authors' knowledge, this was the first use of the Emergency Communications Service for tsunami warning and had a positive impact in the evacuation of the population in Vathi, Samos, where the message according to eyewitnesses was received prior to the second and largest flood. The warning time window gave the opportunity to emergency services to be actively involved in the evacuation, while at the same time, the message dissemination to all cell phones directly warned the population to self-evacuate in an area with limited prior (generational) knowledge of tsunamis.

While tsunami awareness and generational tsunami wisdom (Fritz and Kalligeris 2008; Esteban et al. 2015) are faint in the region, the Aegean has a long history of documented tsunamis in the past two millennia (Ambraseys and Synolakis 2010). The Samos tsunami is arguably the most significant event in the Aegean since the 09 July 1956 Amorgos earthquake and tsunami that produced wave runup values as high as 20 m on the south coast of Amorgos

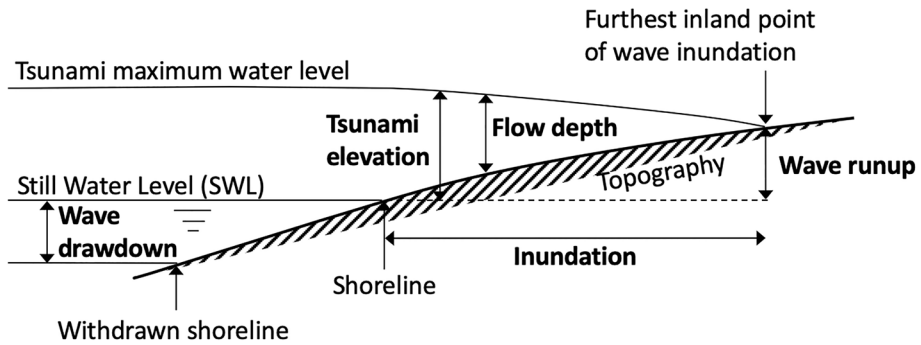


Fig. 2 Diagram showing the terms used for the quantitative measures of tsunami intensity (boldface text) collected at coastal locations during the post-tsunami field surveys

(Okal et al. 2009). It follows four other smaller events that have impacted the Greek coasts since 2017, namely Lesvos on 12 June 2017, Kos on 20 July 2017 (Heidarzadeh et al. 2017; Dogan et al. 2019), Zakynthos on 25 October 2018 (Cirella et al. 2020; Ganas et al. 2020), and south Crete on 02 May 2020 (Heidarzadeh and Gusman 2021). It is also worth noting that a small tsunami was observed along the north coast of Chios island and Cesme, Turkey, following the 23 July 1949 Chios earthquake (Melis et al. 2020). The 30 October 2020 Samos (Aegean Sea) event is yet another reminder of the hazard posed by tsunamis in the region and highlighted once again the tsunami warning challenges posed by near-field tsunamis.

Here, we discuss eyewitness observations and present quantitative runup and overland flow depth measurements and infer a tsunami hydrograph, i.e., a figure which shows the change of the overland flow depth of the tsunami at a particular location. Our field work and our analysis indicate that normal earthquakes with magnitudes not typically associated with perilous tsunamis can cause havoc on waterfronts and may even kill people, who—while nearshore—don't heed the earthquake shaking as a harbinger message to move immediately away from the shoreline.

2 Methodology and instrumentation

We interviewed eyewitnesses of the tsunami and collected quantitative measurements of tsunami impact, per established methods (Synolakis and Okal 2005; UNESCO 2014). Quantitative measurements are useful in characterising the intensity of the generated tsunami, in better understanding the dynamics of impact, and finally as benchmark for hydrodynamic models; a visual description of the quantitative measures of tsunami intensity collected during the field surveys is provided in Fig. 2. From the eyewitness interviews and collected photos/videos—particularly timestamped footage—information can be extracted regarding the arrival time of the first wave, its polarity, as well as the time sequence of the floods. Audio in the videos can be helpful in understanding people's reactions.

The instrumentation used to collect quantitative measurements consisted of a Topcon Hiper Pro Real Time Kinematics (RTK) GNSS system, a 40 m long water level and a levelling rod. The GNSS system was operated in network RTK mode using the nearest available reference station of the URANUS network in Greece (URANUS 2021); the largest baseline distances of ~26 km correspond to the data points collected in Fourni and the NW coast of Samos (Karlovasi and Ag.

Nikolaos). According to the errors provided by the GNSS system, the accuracy of the GNSS-recorded measurements was within ± 3 cm and ± 5 cm in the horizontal and vertical directions, respectively. For the data points collected in the narrow streets of Vathi where the satellite coverage was low, a water-level was used to collect vertical measurements near buildings. The water level is simply a clear plastic tube filled with water through which a horizontal plane of reference can be defined. On one side of the tube, the water level inside the tube matched the height of interest (e.g., a flow depth mark), and on the other side, the reading on a levelling rod (positioned on top of a GNSS-measured point) that matched the water level was recorded. The precision of the vertical difference measurements using the water level is approximately ± 1 cm.

The GNSS system measured orthometric heights using the URANUS geoid model. In each location visited, all elevations measured with the GNSS system were subsequently corrected according to the orthometric height corresponding to the still water level (SWL) at the time of measurement; the date and time the SWL was measured in each location are provided in Table 1 of the Appendix. Since there are no tide gauge data available near the measurement locations, measured elevations were not adjusted to the water level at the time of tsunami impact. In order to assess the influence of the astronomical tide to the water level measurements, the time series of the tidal elevation from the closest grid point of the OSU TPXO9.v4a tidal model (Egbert and Erofeeva 2002) to each measurement location were extracted for the period between 30 October 2020 and 5 February 2021. Due to the absence of detailed offshore and nearshore bathymetry data, the local amplification and dissipation of the tidal wave at the shallow zone and in engulfed areas could not be inferred. Therefore, the tidal range provided in Table 1 of the Appendix for each of the measurement locations is only a qualitative indication of the microtidal regime (Andrew and Cooper 2005) and the associated error in the elevation measurements.

In the town of Vathi, where more detailed tsunami measurements were collected, a drone was used to create a high-resolution orthophoto and a Digital Surface Model (DSM) of the town's waterfront. The drone, a DJI Phantom 4 Pro, was flown at 55 m elevation above ground, capturing images of 5472×3748 pixel resolution. Another, more detailed, drone flight was scheduled at an altitude of 19 m focusing on the building housing the Library of Samos to create a DSM which was used with the tsunami footage frame-by-frame analysis presented in Sect. 4.1. The drone data were post-processed using the Agisoft

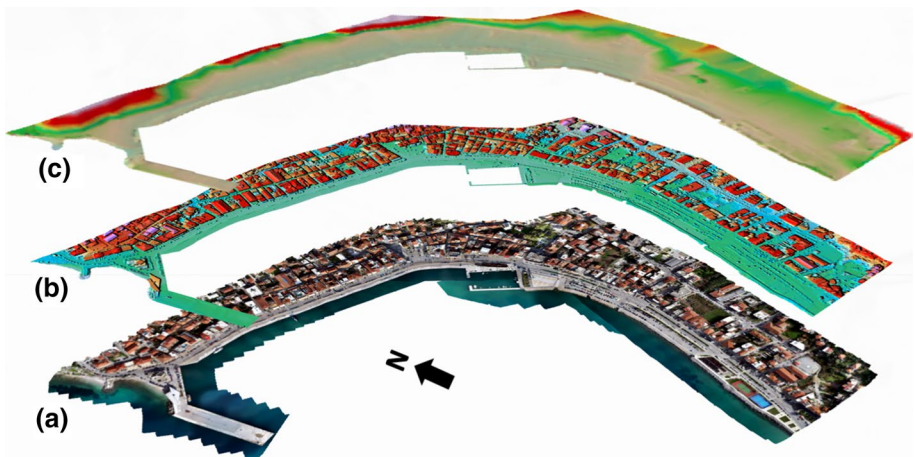


Fig. 3 The orthophoto (a), DSM (b) and bare earth DEM (c) of Vathi created using drone aerial images

Photoscan software to produce high-resolution point clouds, and the data were georeferenced using well-distributed ground control points (GCPs, in the form of targets on the ground) of known world coordinates. The final products were a 5.3 cm resolution orthophoto and DSM of the waterfront of Vathi (Fig. 3), and a 1.7 cm resolution DSM of the Samos Library and its surroundings (Fig. 4). The mean total (xyz) errors of the two DSMs are 3 and 3.7 cm, respectively. The DSM of the waterfront of Vathi was post-processed using ArcGIS Pro tools to create a (bare earth) Digital Elevation Model (DEM) (Fig. 3).

3 Field observations

A post-tsunami reconnaissance team was deployed to the island Samos one day after the earthquake for an initial tsunami impact assessment. Three post-tsunami field survey missions between January and February 2021 followed to collect quantitative measurements of the tsunami impact and interview tsunami eyewitnesses in the Greek islands around the earthquake epicentre, namely the islands of Samos, Chios, Ikaria, Thimena and Fourni. For the surveys, special permits were obtained from the General Secretariat for Civil Protection of Greece, given that the country was on travel restrictions due to the ongoing COVID-19 pandemic. We present an overview of the maximum tsunami runup or tsunami elevation values measured in the field surveys in Fig. 5, while the full list of data points is provided in Table 2 of the Appendix. A description of the findings in each location visited follows below.

3.1 Chios

The E-W orientation of the fault rupture translates to a predominantly N-S tsunami directivity. The island of Chios is located northwest of the fault rupture area, however, the southeast coastline of Chios did receive considerable tsunami energy. Tsunami impact in Chios did not make the mainstream Greek news, as most articles focused on Vathi (Samos), but local news websites (e.g., Astraparis 2020) reported tsunami-induced damage in the harbour of Komi (location C2 in Fig. 5 and Fig. 6a). According to eyewitnesses and local officials, the first wave arrived as a leading depression (Tadepalli and Synolakis 1994), and fishing boats touched the sea floor as the water level dropped. In the flood that followed, which according

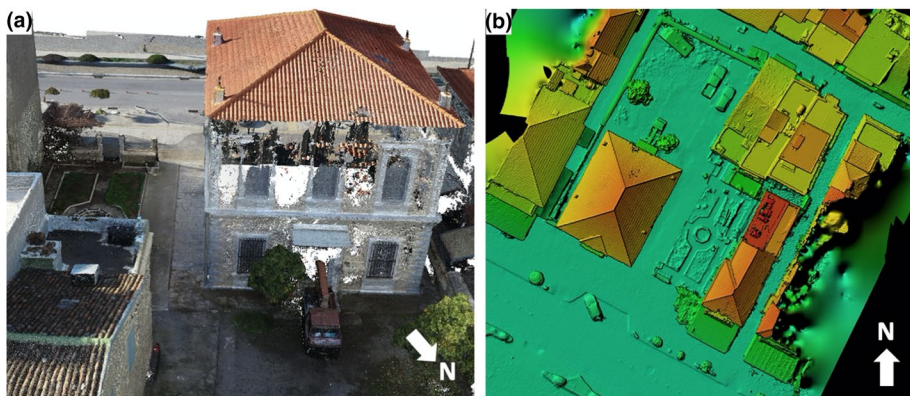


Fig. 4 The point cloud (a) and DSM (b) of Samos Library in Vathi created using drone aerial images

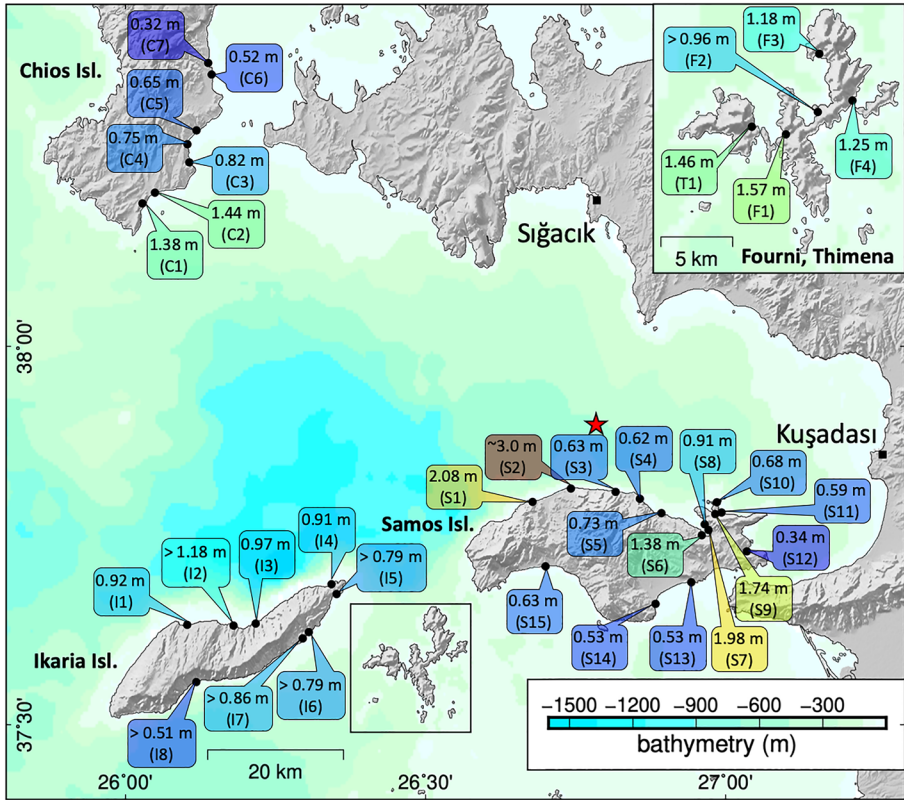


Fig. 5 Overview of the maximum runup and/or tsunami elevation measured in all locations visited in the post-tsunami reconnaissance missions to the Greek islands. Values including the > (greater than) symbol correspond to elevation measurements of structures that were flooded. Since the flow depth on those structures is unknown, the tsunami elevation value corresponds to at least the elevation of the structure. The text balloons are colour-coded according to their respective runup/tsunami elevation value using the “jet” colour map (ranging from 0 to 3 m, 0 being blue and 3 being red). The coloured background shows the GEBCO bathymetric relief (GEBCO 2020) and the red star corresponds to the USGS earthquake epicentre

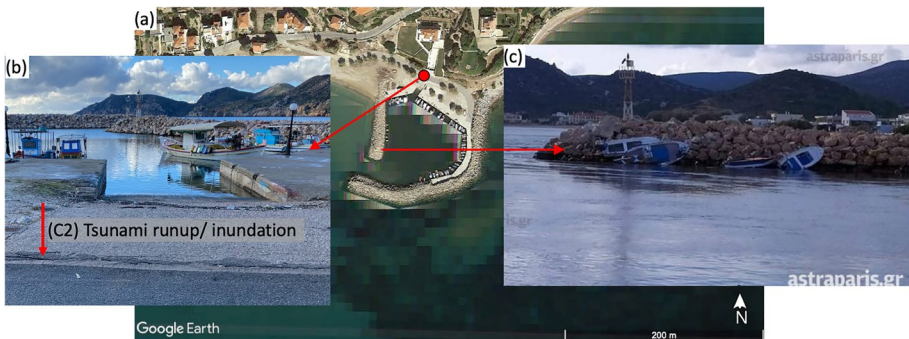


Fig. 6 **a** Google Earth satellite picture of Komi and the location of the runup/inundation measurement. **b** A picture from the field showing the maximum runup/inundation point measured north of the harbour slip. **c** A picture from a news article showing the fishing boats that were dragged by the tsunami-induced currents to the side of the breakwater (source: Astraparis 2020)

to eyewitnesses was the largest observed, the water overtopped the harbour dock and reached the coastal road at ~ 1.46 m of elevation (Fig. 6b). The mooring lines of some of the fishing boats broke or came off and the tsunami-induced currents dragged and deposited them on the harbour side of the breakwater (Fig. 6c). While the tsunami impacted the harbour, the waves didn't reach any of the houses sitting on the beach adjacent to the harbour.

In the small bay and town of Emporios (location C1), located ~ 2 km SW of Komi, three significant tsunami-induced floods were observed by an eyewitness. The first and largest flood was described as having "momentum" and inundated the coastal road of the town, reaching 1.4 m of elevation, penetrating ~ 60 m inland. Tsunami amplitude gradually decayed moving north of Komi, along the coast. Tsunami observation locations are limited to small harbours where tsunami amplitude was amplified, but the water level fluctuations did not cause any damage. The waves overtopped the dock only in the harbour of Katarraktis (location C4), with an additional ~ 5 cm of flow depth, but the water level rise was described as "gradual" and didn't cause any damage. In the port of Chios (location C7), where the northernmost data point was collected, only people observing the sea were able to identify any tsunami effects and pointed us to a maximum tsunami elevation reaching ~ 0.3 m (data point C7). The authors were not able to collect any timestamped pictures or video of first wave arrival in any of the locations visited in Chios.

3.2 Ikaria

Eyewitness accounts and CCTV footage show that the tsunami arrived in both the northern and southern coast of Ikaria as a leading depression wave. From the map in Fig. 5, it is evident that the maximum tsunami elevation/runup data points recorded in the field survey were generally higher on the north coast compared to the south. Reports of tsunami sightings have mainly focused on the two main ports of the island, namely Evdilos (location I2) on the north coast, and Ag. Kirikos (location I7) on the south coast, which is also the administrative capital of Ikaria. CCTV videos from cameras overlooking the two ports (YouTube, 2020a, 2020b) show the water level dropping first at $\sim 11:57$ and $\sim 12:02$ UTC at Evdilos and Ag. Kirikos, respectively (after correcting the clock time based on the earthquake shaking initiation). The first, third and fifth floods appear to be the largest in Evdilos, whereas the second and fourth floods appear to be the largest in Ag. Kirikos. In both locations, the maximum floods are seen just overtopping certain harbour docks that were measured in the field survey, but no major damage was reported. The periodicity of the fluctuations deduced by the CCTV videos is on average ~ 6 and ~ 3 min in Evdilos and Ag. Kirikos, respectively.

Elsewhere in Ikaria, the maximum runup did not reach any of the buildings located near the shoreline and the tsunami effects were mostly noticeable in harbours, where no significant damage was reported. The only additional timestamped footage collected, apart from the publicly accessible CCTV videos for the two main ports, were provided by an eyewitness in the harbour of Ag. Kiriaki (location I4), which is located on the north coast, right west of the airport runway. The video in Ag. Kiriaki shows a flood peaking at $\sim 12:25$ UTC, which according to the eyewitness corresponds either to the third or fourth wave in this location.

3.3 Fourni

Eyewitnesses in the main town of Fourni (location F1) reported the first wave as a leading depression. The shoreline withdrawal at the beach next to the harbour and water level depression along the harbour docks were quickly noticed by locals. Upon associating the

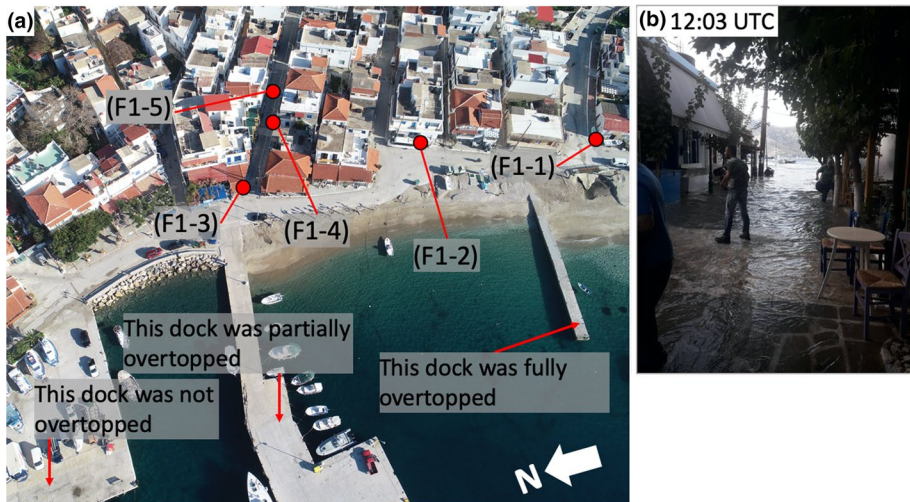


Fig. 7 **a** Aerial picture of the town of Fourni showing the locations where tsunami field measurements were collected and revealing the coastline features described in the text. **b** A timestamped eyewitness picture of the main commercial street of Fourni being flooded by the first and largest wave (photo credit: A. Chalaros)

depression with the earthquake, and realising the imminent threat of a flood, the local coast guards quickly gave orders to evacuate people from the waterfront. The first flood peaked around 12:03 UTC, which was inferred from an eyewitness timestamped picture (Fig. 7b) and video. The maximum sea level reached in Fourni overtopped an older low-lying dock (southernmost dock in Fig. 7a), partially flooded another, but did not overtop the higher-elevation newer dock (Fig. 7a). The water penetrated inland through the beach, but also through wall openings, drains, and coastal features of lower level topography.

Maximum runup was measured along the main commercial town street (data point F1-5), which at the time of writing did not appear to have a name. An additional runup and three tsunami elevation points were collected in the town of Fourni as indicated by eyewitnesses. The residents mentioned at least two additional floods in Fourni, but that the first was the largest. A timestamped video captured at 12:14 UTC shows that the water level was rising and had already flooded the coastal road, while a picture taken at 12:31 UTC shows another flood event. There was no substantial damage due to the tsunami in the town of Fourni, which was described as a fast-rising tide with no significant overland flow velocity. The data points collected in other locations along the northern part of the island of Fourni (data points F2-F4) show consistent runup/tsunami elevation values above 1 m, but no flooding of any coastal buildings was reported.

3.4 Thimena

The town of Thimena (location T1) on the namesake island features a small harbour (Fig. 8a) and is located ~2.3 km to the west of the town of Fourni. According to several eyewitnesses, the tsunami arrived as a leading depression wave, and during the drawdown phase some fishing boats touched the sea floor. The (first) flood that followed was described as being the largest. An eyewitness video shared with us that was filmed at 12:07 UTC,



Fig. 8 **a** Aerial picture showing the harbour of Thimena, and the tsunami elevation data point measured on the first step of the staircase connecting the harbour to the town (**b**). **c** A frame from an eyewitness video showing an eddy forming at the corner of the harbour dock during the second drawdown phase and the harbour docks being already flooded

shows an eddy forming at the eastern corner of the harbour dock (Borrero et al. 2015; Kalligeris et al. 2016, 2021), presumably during the second drawdown phase, and the harbour docks appear to have been previously flooded (Fig. 8c). The overtopping of the docks during the first (and largest) flood was also confirmed by eyewitnesses, who described a flow depth over the dock between 15–20 cm; the harbour docks were not overtopped during any of the subsequent floods. Eyewitnesses pointed to a staircase that connects the harbour with the town and described how the maximum water level reached the first step, which was the data point recorded in this location (Fig. 8b). According to a local eyewitness, the tsunami had a much smaller amplitude in the small town of Keramidou.

3.5 Samos

Being the most heavily impacted island from the earthquake and tsunami, Samos became the main focus of the field survey. Data points were collected from fifteen coastal locations on the north, east and south sides of the island. On the southern coast, moving from east to west, we visited Pythagorion (location S13), Ireo (location S14) and Marathokampos (location S15), with measured runoff/tsunami elevation values being below 0.65 m. In Ireo and Marathokampos, eyewitnesses described a leading depression wave, while in Pythagorion eyewitnesses were not able to provide wave polarity information. Timestamped eyewitness pictures taken in Marathokampos show that at 12:12 UTC the shoreline on a beach inside the local harbour had already receded. No damage due to the tsunami has been reported on the south side of Samos.

On the east and northeast side of Samos, we visited Charavgi (location S12) and Ag. Paraskevi (location S11). In Ag. Paraskevi, the eyewitness we interviewed described the first wave arriving ~30 min after the earthquake as a leading elevation, whereas in

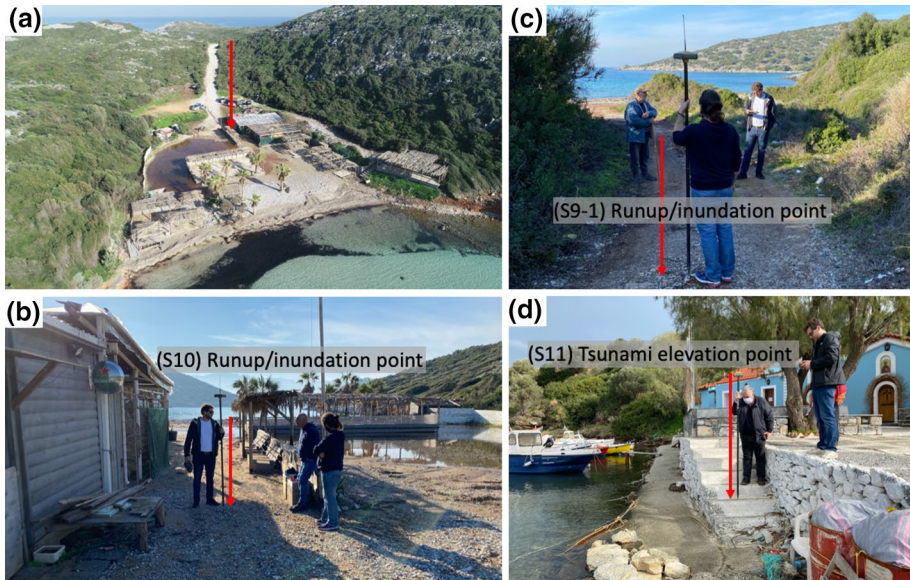


Fig. 9 **a–b** Aerial and ground picture of the runup/inundation point collected in Livadaki, Samos. **c–d** The runup/inundation and tsunami elevation points collected in Asprochorti and Ag. Paraskevi, respectively

Charavgi the eyewitnesses described a leading depression first wave arrival. The maximum tsunami elevation reached in Charavgi was indicated by eyewitnesses on a wooden jetty, whereas in Ag. Paraskevi at a staircase on the local harbour dock (Fig. 9d). Moving north of Ag. Paraskevi, the bay and beach of Livadaki (location S10) are sitting at the northeastern tip of Samos. The owner of the local business in Livadaki drove to the beach about an hour after the earthquake and recognised the wrack line left by the wave runup next to a beach shack (Fig. 9a–b). The measured wave runup of 0.68 m is significantly lower than the data point collected in Asprochorti (location S9), sitting at the end of a northwest-facing narrow bay, ~ 1.7 km south of the beach of Livadaki. In Asprochorti, a local resident witnessed a leading depression wave and three “significant” floods, each being larger than the previous one. Wave runup from the third flood reached 1.74 m (Fig. 9c), which is comparable to the wave runup measured in Vathi, both places being located at the end of narrow bays on the north-eastern side of Samos.

On the north-western side of Samos, we visited the port and town of Karlovasi (location S1), and the coastal town of Ag. Nikolaos (location S2). In Karlovasi, two time-stamped pictures were shared by an eyewitness in the boat maintenance area of the port taken during the initial drawdown phase (data point S1-2) and shortly after maximum runup of the first flood (Fig. 10b–c). We found another picture taken at 11:58 UTC shortly after the first flood peaked in front of the Hellenic Coast Guard building and when the water level was dropping, with the water level being at 1.66 m with respect to the SWL; all three were key in identifying the timing of tsunami impact. The four runup points measured as indicated by eyewitnesses are consistent with a > 1.8 m wave runup in Karlovasi, which is comparable to the maximum runup recorded in Vathi. However, flooding was limited in Karlovasi, primarily due to the high elevation of the port docks, which also resulted in a smaller flow depth compared to Vathi. In Karlovasi, only the

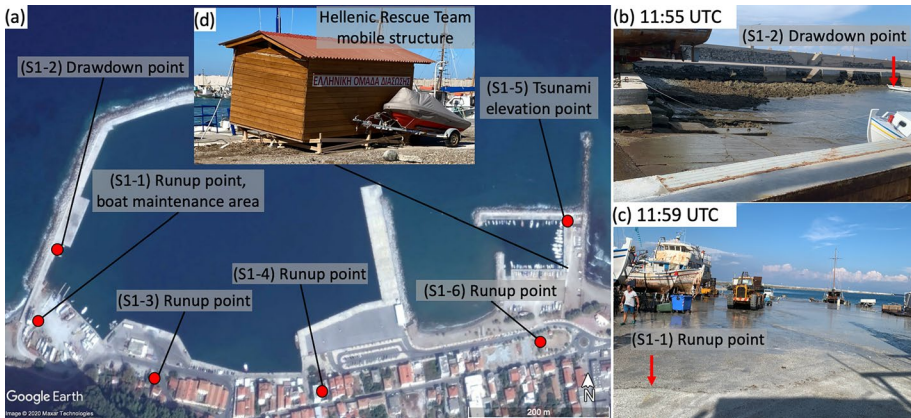


Fig. 10 **a** Google Earth satellite picture of the port of Karlovasi and the locations of tsunami observations. **b–c** Eyewitness pictures of the initial wave drawdown and subsequent runup captured at the boat maintenance area shortly after the earthquake (photo credit: A. Spanogiannis). **d** The mobile structure of the Hellenic Rescue Team that was displaced by the tsunami

first-row buildings facing the waterfront on the western side of the port were flooded by the tsunami and no major damage was reported. A mobile structure of the Hellenic Rescue Team resting on top of a supporting wooden frame, right next to the dock of the marina was most likely uplifted by the overland flow and displaced, leading to some small damage to the wooden frame (Fig. 10d).

In Ag. Nikolaos (location S2), the authors were provided with the CCTV footage shared in social media that shows a coastal residence being impacted by the tsunami (YouTube, 2020c). Figure 11 depicts four frames extracted from the video that contain important

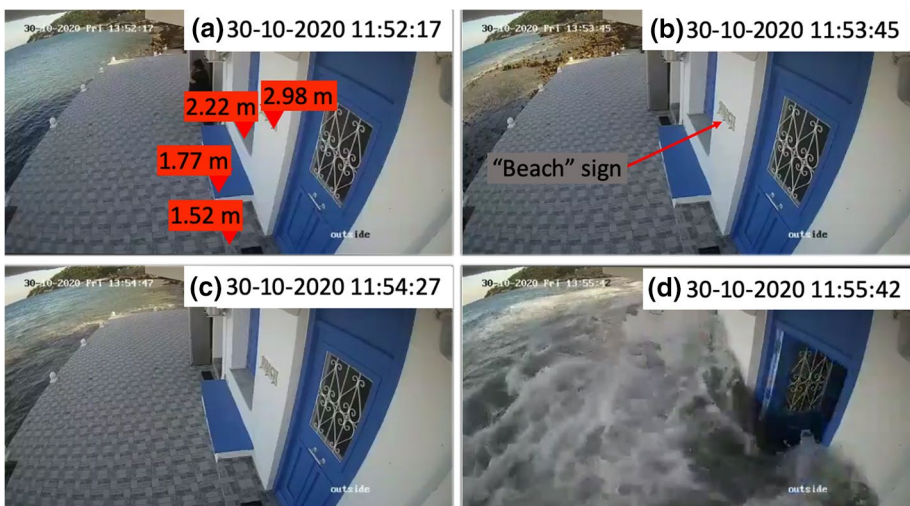


Fig. 11 **a–d** Frames from a CCTV video captured in a coastal residence of Ag. Nikolaos, Samos; date and time displayed is UTC. The elevations (above SWL at the time of measurements) of various features of the building facade are displayed in (a)

information for the timing of impact: the shoreline withdraws (Fig. 11b), the sea level rises and peaks (Fig. 11c), and the last frame (Fig. 11d) shows the impact of a subsequent flood. The steep wave front that impacts the coastal residence appears more violent compared to any other coastal location for which video footage is available for the Samos (Aegean Sea) tsunami, and is seen arriving from the east, propagating westward along the coast. Upon visiting this location and measuring the elevation of the distinct features on the house's facade (Fig. 11a), it can be safely said—excluding the water splash—that the tsunami elevation in this location reached at least 2.22 m above SWL (windowsill), and was below ~3.0 m (the lower side of the “Beach” sign).

The first harbour ~6.5 km east from Ag. Nikolaos on the north coast of Samos is Ag. Konstantinos (location S3). A local eyewitness described first noticing the sea level rising and pointed to a certain step on the dock reached by the maximum tsunami elevation which measures at 0.63 m above SWL (data point S3), which was confirmed by another eyewitness. Further east, at Avlakia (location S4), an eyewitness described that the third wave was the largest and ran up to a point we measured at 0.62 m above SWL (data point S4). In Kokkari (location S5), the eyewitness we interviewed first noticed the water level rising ~15 min after the earthquake and pointed to the maximum runup point at the end of a small beach inside the local harbour, which measures at 0.73 m above SWL (data point S5). Thus, all coastal locations along the coastal stretch between Ag. Konstantinos and Kokkari received significantly less tsunami energy compared to Ag. Nikolaos.

In the bay of Vathi, three locations were surveyed, namely Gaggos beach (location S8) on the northeast side of the bay, Malagari on the west (location S6), and the town of Vathi (location S7) located at the end of the bay. In Gaggos beach, two eyewitnesses described that the shoreline started receding about 10 min after the earthquake and the flooding was repeated every ~10 min. A wrack line with small debris was still recognisable on the beach on the day of our visit (data point S8), while another runup/inundation point indicated by an eyewitness matched the runup height corresponding to the wrack line. In Malagari, we interviewed several eyewitnesses along the coast. A runup/inundation point was collected on the north side, as indicated by an eyewitness/local resident, who following the earthquake rode his motorbike along the dirt road that connects his business to the coastal road and saw the sea advancing. Further south, around the boat parking/maintenance area, we collected two data points. The first was based on the interview with a local resident who indicated that the maximum water level reached the first step at the entrance to her residence. A runup/inundation point was indicated by another eyewitness in the parking lot area of his business. At the same location, CCTV footage was shared with us from a camera overlooking the boat parking area. The video shows that the water level started rising at 12:23 UTC (after correcting the clock time based on the earthquake shaking initiation) and reached its maximum level at ~12:27 UTC (Fig. 12a–b). The southernmost data point collected in Malagari was indicated by an eyewitness who went to higher ground after the earthquake and identified the maximum inundation point when he came back to his business soon after.

The town of Vathi, the largest town in the island of Samos, was the hardest-hit location in the Greek archipelago. The tsunami reached the first two–three building blocks along the waterfront of Vathi and flooded basements and ground floors of businesses and residential buildings (Fig. 13). The overland flow depth exceeded 1 m in certain locations of lower elevation, causing extensive property damage to the local retail sector. Being located at the end of Vathi bay, and also further away from the fault rupture area, tsunami arrival was delayed compared to Karlovasi. The tsunami arrived as a leading depression wave and the first flood started at ~12:04 UTC. Following the first flood, the message from the Secretariat for Civil

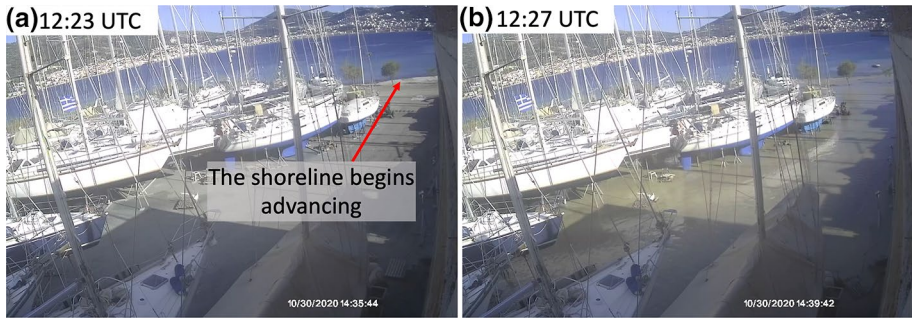


Fig. 12 CCTV footage frames from the boat parking area in Malagari, Samos, showing the moments when (a) the shoreline started advancing and (b) when the flood peaked (UTC times shown were corrected based on the earthquake shaking initiation)



Fig. 13 a–c Eyewitness pictures from the second and largest flood in Vathi, Samos. d A characteristic flow depth point identified on a dusty shopping window the day after the tsunami along Tompazi St. in Vathi (data point S7–12)

Protection of Greece through Greece's 1–1–2 Emergency Communications Service was received on cell phones in Samos. The message warned people to stay away from the coast following the earthquake and, importantly, was received prior to the second and largest flood. It is worth noting that emergency response authorities reported soon after the event that the 1–1–2 emergency message was received prior to the first flood; this implies that due to its smaller amplitude compared to the second flood, the first flood was either unnoticed in areas of higher elevation or was not perceived as of any significance.

The following section presents extensive field measurements and video analysis in Vathi to shed light on the local sequencing and impact of the tsunami.

4 Detailed field observations in Vathi, Samos

In Vathi, we undertook a detailed survey and collected 33 data points. The majority was identified through eyewitness interviews, while a small number of points were either visible flow depth marks or were inferred through eyewitness videos. Figure 14a presents an overview of

the locations and types of data points collected in Vathi; the data point elevations can be identified through the top and side plots. Figure 14c–i show selected topography cross profiles normal to the shoreline, extracted from the DSM, with the maximum water level inferred from the nearest field data, as well as from eyewitness and CCTV footage.

Moving from NW to SE along the shoreline until reaching the marina, the elevation of the harbour quay decreases from 0.68 m to 0.4 m above SWL (transects T1–T4). The vulnerable sections of the waterfront in Vathi between T2 and T4, were impacted by both the first and second waves. Pythagoras square was partially flooded by the first wave and was completely flooded by the second and largest wave. During the second flood, the water travelled through the square and also along section T3 to reach Ag. Nikolaos square from two sides, where we measured a wave runup of 1.91 m and the largest inundation distance of 108 m (data point S7-20). On the SE side of Pythagoras square, the water climbed on commercial Ag. Nikoao St., where the water ran up to 1.98 m, the highest runup measurement in Vathi (data point S7-17). The second flood also significantly impacted the commercial Cpt. Stamatis St, where flow depth was as high as 0.7 m on the southern end, while on the northern end the wave ran up to 1.77 m (data point S7-15). Interestingly, maximum wave runup along Kyrillou St. was measured at 1.59 m (data point S7-16) – runup data points S7-15 and S7-16 along the two intersecting streets indicated by eyewitnesses were 13 m apart.

South of the marina, a rip-rap breakwater apparently reduced the impact of the tsunami. From its northernmost extent until cross profile T6, the elevation of the breakwater was below the maximum water level reached in the second flood. Albeit briefly, that section of the breakwater was overtopped, and wave overtopping contributed to the flooding mostly in the lower-topography areas near the breakwater (see cross profiles T5–T6).

The furthest south business to be flooded by the tsunami was a storage room along cross profile T6 (southernmost data point S7-1). The source of flooding in that area, which approximately constitutes the south limit of the alongshore tsunami inundation in Vathi, was very complex. Figure 14b, h, i show how wave inundation propagated southwards through the lower topography along the shore-parallel street and the breakwater was overtopped when the offshore water level peaked (the waves did not overtop the breakwater south of cross profile T6). Sea water was also flowing out of the storm drains through hydrostatic pressure while the offshore water level was higher than the elevation of the storm drains.

The discharge of water through the storm drains depended not only on the elevation of the storm drains, but also on the size of the storm drain pipes and their outlets in the sea. Cross profile T5 (Fig. 14g) runs along one of the storm drain pipes and outlets. The back flow through the storm drainpipe due to hydrostatic pressure was such that the pavement next to the storm drain collapsed (local depression in T5 captured by the DSM), leading to higher discharge rates. This effect likely caused a local increase in the tsunami elevation—refer to side plot of Fig. 14a.

4.1 Video analysis

The sequencing, timing, water elevation and surface velocities of flood events in Vathi were interpreted through CCTV footage shared with us from two buildings along the waterfront: Samos Library and the Rhenia Tours travel office; video analysis has been done for other past tsunamis to extract water levels and current velocities (Fritz et al. 2006, 2012, 2018; Kalligeris et al. 2016). The travel office CCTV footage overlooking the business entrance on the waterfront covers 2 h and 37 min. after the earthquake and captures five flood events. Figure 15 shows the frames from the travel office footage at

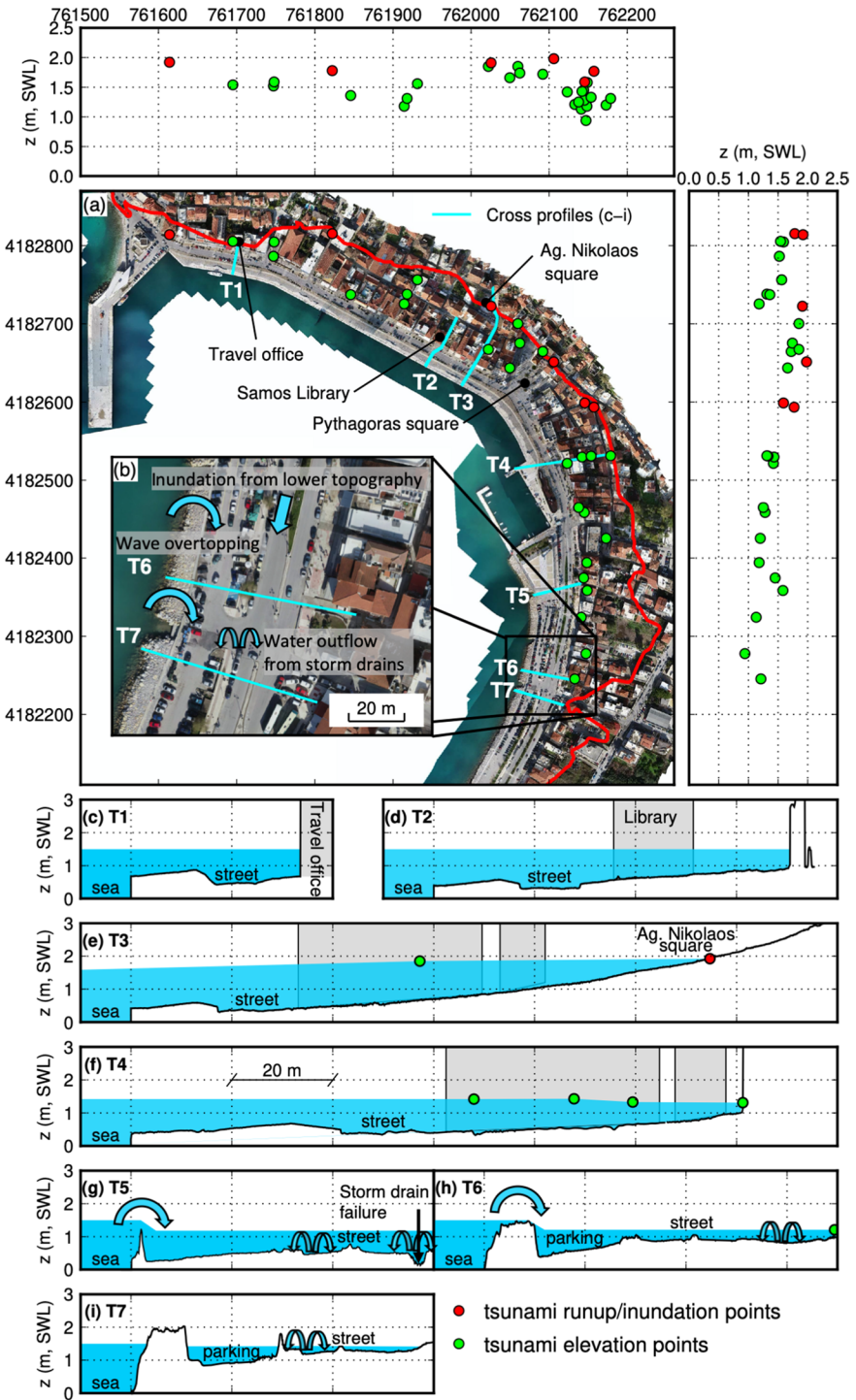
Fig. 14 **a** Tsunami runup/inundation and elevation points overlaid over the orthophoto of Vathi, Samos, referenced to the (projected, units in meters) 1987 Greek Geodetic Reference System (GGRS87); the red curve corresponds to the 2 m topography contour extracted from the bare earth DEM model and the cyan lines show the top view of the cross profiles plotted in c-i. **b** Inset figure at the southern limit of tsunami inundation in Vathi, showing the multiple flooding routes. **c–i** DSM topography cross profiles (black lines) and corresponding maximum tsunami elevation (cyan-coloured envelope) inferred from the measured tsunami data points, and eyewitness and CCTV video footage

the time each flood event reached its maximum elevation. The maximum water elevation reached in each flood displayed in Fig. 15 was inferred through objects seen in the image whose elevations were surveyed, in combination with the high-resolution DSM of Vathi created using the drone images. It is important to stress that in this location only the second and fourth waves overtopped the concrete structure located between the harbour quay and the street, while in the other events the water flooded the street and pavement through areas of lower topography and the storm drains (located at ~ 0.44 m above SWL). As a result, for the flood events that didn't overtop the concrete structure, flooding was delayed, and the maximum water level was deficient compared to other locations impacted directly through wave overtopping.

Samos Library has several security cameras mounted on the perimeter of the building. The two cameras that are of particular interest to this study are the one overlooking the library entrance on the waterfront, and the camera that overlooks the lane on the side of the building leading to the parking area in the back, labelled *cam1* and *cam2* in Fig. 16a, respectively. The library videos, covering the first two floods, were used to extract overland tsunami height and free surface velocity time series.

Tsunami elevation time series were extracted from the *cam1* videos of the first two floods simply by placing a levelling rod at a corner of the Samos Library facade next to the entrance (Fig. 16b). At each video frame, the water level reached on this corner of the building as seen in the video was translated to tsunami elevation by reading the corresponding levelling rod values and adding the ground elevation with respect to the still water level (SWL) at the time of measurements. The resulting tsunami elevation time series extracted from the videos are shown in Fig. 17a–b. The first and second floods peaked at just over 1 and 1.5 m above SWL, respectively. In comparison with the timing and maximum elevations extracted from the travel office CCTV footage, the maximum water level of the first flood was reached earlier at the library ($\sim 12:05:50$ UTC at the library versus $\sim 12:08:03$ at the travel office) and had a higher elevation compared to the travel office (~ 1.05 m at the library versus ~ 0.6 m at the travel office). The elevation of the cross section between the shoreline and the street is lower at the library compared to the travel office (compared cross profiles in Fig. 14c–d) and as a result, it was overtopped by the first wave only at the library and not at the travel office.

The *cam2* footage was used to extract free surface velocities for the second and largest flood in Vathi using the same methodology as described in Kalligeris et al. (2016). Optical tracing requires to determine the camera intrinsic (camera and lens properties) and extrinsic (camera location and orientation) parameters. For the camera intrinsic parameters, only radial and decentering lens distortion parameters were recovered through straight line objects appearing curved in the image using the methodology outlined by Swaminathan and Nayar (2000). The camera extrinsic parameters were defined through the Direct Linear Transformation (DLT) coefficients L_p , $i = 1, 2, 3, \dots, 11$ (Holland et al. 1997). The best-fitting DLT coefficients were recovered by rewriting the relationship between image and world coordinates as a system of linear equations of the



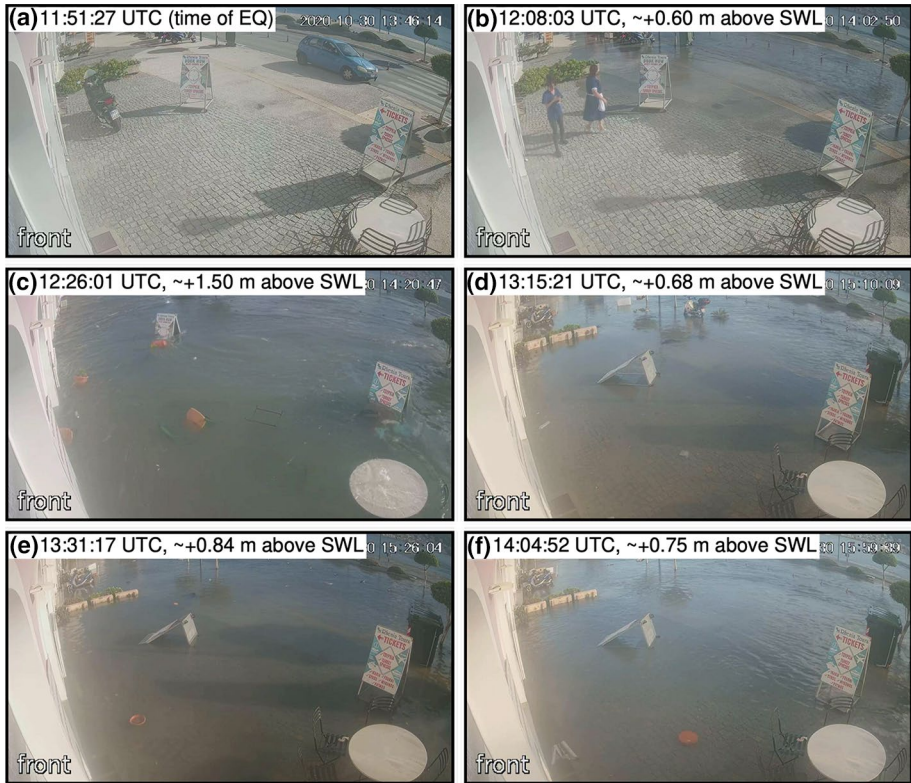


Fig. 15 Video frames extracted from the travel office CCTV footage showing the (corrected) times and maximum elevations reached by the individual tsunami-induced floods in this location of Vathi, Samos

form $\mathbf{A} \cdot \vec{x} = \vec{b}$ and using the seven non-coplanar ground control points (GCPs) shown in Fig. 16c whose world coordinates were obtained from the Library high-resolution DSM (Fig. 4). Reconstructing the world coordinates of the GCPs from their (undistorted) image coordinates using the best-fitting DLT coefficients yields a mean horizontal error of 1 cm.

After optically tracing various floating objects identified in the video, the tracer paths in image coordinates (u , v) were translated to world coordinates (x , y) using the DLT coefficients as (Kalligeris et al. 2016):

$$\begin{bmatrix} x \\ y \end{bmatrix} = \begin{bmatrix} L_1 - L_9 u \\ L_5 - L_9 v \end{bmatrix} \begin{bmatrix} L_2 - L_{10} u \\ L_6 - L_{10} v \end{bmatrix}^{-1} \begin{bmatrix} u - L_4 + z_t (L_{11} u - L_3) \\ v - L_8 + z_t (L_{11} v - L_7) \end{bmatrix} \quad (1)$$

where z_t is the tracer elevation, which was independently estimated. After the flood peaked, the tracer level z_t was set equal to the water level at the building facade extracted from the *cam1* video analysis. Due to the narrow width of the entrance through which the water was rushing from the waterfront to the lane on the side of the building, the water level on the side of the building was not equal to the water level on the waterfront before the flood peaked. The water level for two optically tracked objects, appearing in the footage before

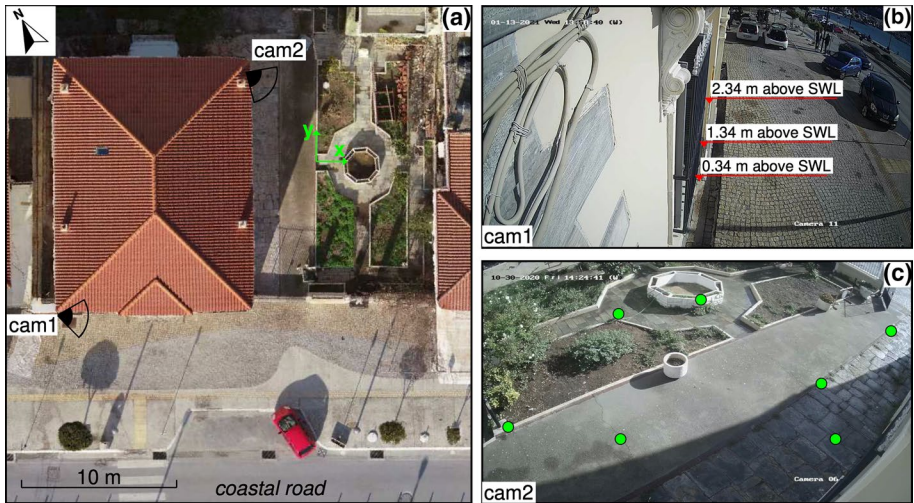


Fig. 16 **a** The location and orientation of the two cameras (*cam1* and *cam2*) used to extract overland tsunami heights and free surface velocities overlaid on an orthophoto of Samos Library; the local coordinate system used with the free surface velocities overlaid is shown with the green arrows, x and y being the shore-parallel and shore-normal directions, respectively. **b** The field of view of *cam1* showing the levelling rod placed on the corner of the building facade to extract water level information; reference heights are provided. **c** The field of view of *cam2* and the ground control point (green circles) through which the camera extrinsic parameters were determined

the flood peaked, was inferred through features of known dimensions that were partially flooded. For the world coordinates (x , y), a local coordinate system was defined where the x and y axes are parallel and normal to the shoreline, respectively (Fig. 16a).

The tracer paths in world coordinates extracted with the 25 Hz sampling frequency were first filtered using a low-pass Butterworth filter with 2.5 Hz cut off frequency to remove high frequency fluctuations due to optical tracing errors and local water level fluctuations. The filtered paths (Fig. 17e) were then translated to velocities using the first order central difference scheme. The resulting shore-normal velocities and corresponding velocity magnitudes are shown in Fig. 17c–d. Each tracer, plotted using a different colour, experienced high acceleration/deceleration as it moved through the camera field of view in regions of varying velocity as is evident from the steep individual velocity curves. Free surface velocities as high as 2.5 m/s were measured as the flow depth reached ~ 0.83 m, which corresponds to a subcritical flow according to the Froude number ($Fr < 1$) using the mean ground elevation in the optical field of view $h = 0.68$ m. The video frames shown in Fig. 17f–g indicate supercritical flow conditions before the second flood peaked.

5 Discussion and conclusions

We described our results from several post-event field surveys we undertook. In Chios, the SE shoreline between Emporios and Komi received most of the tsunami energy, with 1.44 m of wave runup measured in Komi, while the wave amplitude faded moving north

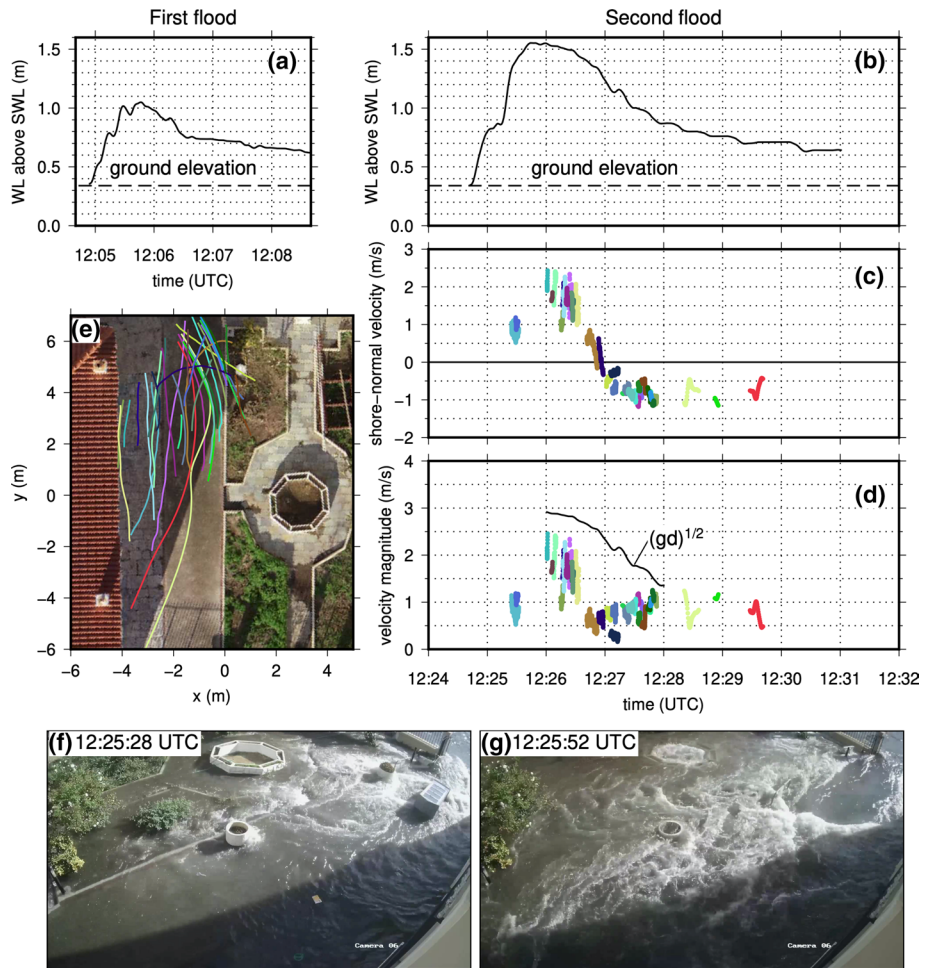


Fig. 17 **a–b** Tsunami elevation time series of the first two floods in Vathi extracted from the *cam1* Samos Library CCTV video. **c** Shore-normal free surface velocities for the second flood in Vathi extracted from the *cam2* Samos Library CCTV video through particle tracking; each colour corresponds to a different particle. **d** Same as (c), but showing the velocity magnitude; the black curve corresponds to the shallow water speed \sqrt{gd} , where d is the flow depth computed by subtracting the mean ground elevation in the optical field of view ($h = 0.68$ m) from the water level d extracted from (b) after the flood peaked. **e** The paths of the objects optically tracked, projected on top of an orthophoto. **f–g** Two frames of the *cam2* footage for the second flood showing the flow conditions during the flood rise stage

along the shoreline towards the port of Chios. In Chios and Ikaria, the tsunami was mostly noticeable in ports and harbours justifying the Japanese term. Along the north coast of Ikaria, runup ranged between 0.9 m and 1.2 m, while along its southern coastline maximum measured runup was below 1 m. Provided the timing correction of the published CCTV footage for the tsunami in Evdilos (YouTube, 2020b) is accurate, the tsunami arrived to the north coast of Ikaria as a leading depression wave within 10 min after the earthquake.

In the islands of Fourni and Thimena, the measured maximum runup values of 1.57 and 1.46 m, respectively, were perhaps surprisingly high given the location of the islands with respect

to Samos and the fault rupture area. The relatively early arrival time of the first flood in both towns of Fourni and Thimena (12:03 UTC in Fourni and before 12:07 UTC in Thimena) is another factor that puts a question mark on the origin of the first and largest wave in these locations.

In Samos, the southern and eastern coastlines received significantly less wave energy than the north side and the tsunami was mostly noticed in harbours. Maximum measured runup/elevation values ranged between 0.34 and 0.63 m, while the arrival of the leading depression wave at 12:12 UTC inferred from eyewitness pictures in Marathokampos is noteworthy.

In the NW coast of Samos, located very close to the outcrop of the fault rupture area, the first wave arrived as a leading depression within a few minutes after the earthquake in Karlovasi and Ag. Nikolaos. Wave runup in Karlovasi was consistently measured close to ~2 m, and the town was spared from significant flooding because of the relatively higher topography compared to Vathi. In Ag. Nikolaos, a CCTV footage shared in news and social media shows a steep wave propagating from east to west and impacting a coastal residence, with tsunami elevation reaching values above 2.22 m (~3 m when considering the splash on the wall). In Ag. Konstantinos, located ~6.5 km east of Ag. Nikolaos, tsunami runup/elevation drops to 0.63 m. Such a steep alongshore runup decay is characteristic for landslide tsunamis (Okal and Synolakis 2004). If that is indeed the case, the origin of the submarine landslide may possibly lie just east of Ag. Nikolaos, in an area that features steep bathymetric inclines (Nomikou et al. 2021).

In Vathi bay, recorded maximum wave runup increased from 0.91 m in Gaggos beach to 1.98 m in the town of Vathi located at the end of the bay—comparable maximum runup (1.78 m) was measured in Asprochorti which is located ~2.5 km NNE of Vathi, at the end of another, smaller and narrower bay. Vathi is the capital of the municipality of East Samos and the largest town of the island. Due to its location at the end of the bay, its low elevation and vulnerable waterfront, it was the hardest hit coastal location in the Greek islands. CCTV footage at the waterfront shared by a local travel office showed that at least five waves impacted Vathi, the second being the largest. We presented detailed measurements of tsunami elevation and wave runup along the impacted region, accompanied by drone-extracted topographic cross profiles that showcase the vulnerability of the waterfront of Vathi and the complexity of flooding through multiple routes. Analysis of CCTV footage from the Library of Samos revealed the tsunami hydrographs of the first two floods, i.e. time series of overland flow depth of the tsunami at the particular location, as well as overland flow velocities through particle tracking velocimetry. The hydrograph of the second flood shows that the overland flow depth rose by one meter within one minute.

The message disseminated by the General Secretariat for Civil Protection of Greece through the national 1–1-2 Emergency Communications Service, warning recipients to stay away from coastal areas, was the biggest take away from this event. It was received in Vathi prior to the second and largest flood and according to local officials had a positive effect in the evacuation of the population. Given this promising outcome, future use of this technology for tsunami warning shall be examined. However, raising tsunami awareness of the population to self-evacuate remains the main priority, given that the earthquake itself provides the clearest natural warning in the near-field and it can save lives.

Appendix

See Tables 1 and 2.

Table 1 Water level (WL) measurements collected and tidal model predictions (statistics for the time period between 30 October 2020 and 5 February 2021) for all locations visited

WL measurements							Tidal model		
Island	Location	Date	Time (UTC)	Lon (deg)	Lat (deg)	Nearest cell depth (m)	Min. amp. (cm)	Max amp (cm)	
Chios	Komi	14/1/21	9:03	26.048974	38.20196	54	-10.1	8.7	
Chios	Emporios	14/1/21	9:57	26.028846	38.18812	66	-10.3	8.9	
Chios	Vokaria	14/1/21	11:17	26.106569	38.24169	73	-10.1	8.7	
Chios	Katarraktis	14/1/21	11:37	26.10324	38.26552	49	-10.3	8.9	
Chios	Ag. Ioannis	14/1/21	13:05	26.11825	38.28363	38	-10.6	9.1	
Chios	Farkena	14/1/21	15:25	26.143462	38.35705	9	-13.0	11.4	
Chios	Chios Port	14/1/21	17:10	26.137479	38.37173	9	-13.0	11.4	
Ikaria	Magganitis	18/1/21	12:18	26.117641	37.55696	473	-6.9	6.2	
Ikaria	Fanari	18/1/21	14:49	26.35177	37.67302	55	-7.5	6.2	
Ikaria	Ag. Kiriaki	18/1/21	15:01	26.34355	37.6864	76	-9.1	7.6	
Ikaria	Therma (also applied to Ag. Kirikos)	19/1/21	14:18	26.305627	37.62312	94	-6.9	6.0	
Ikaria	Karavostomo	19/1/21	10:55	26.218245	37.63424	42	-9.2	7.8	
Ikaria	Gialiskari	19/1/21	11:52	26.102734	37.63237	50	-9.2	7.9	
Ikaria	Evdilos	19/1/21	12:35	26.180024	37.63101	32	-9.2	7.8	
Fourni	Fourni	20/1/21	9:25	26.479776	37.57789	147	-7.5	6.5	
Fourni	Bali	20/1/21	10:53	26.505687	37.5918	114	-7.8	6.6	
Fourni	Kamari	20/1/21	11:21	26.532789	37.59866	106	-7.8	6.7	
Fourni	Chrisomillia	20/1/21	12:05	26.507986	37.6269	96	-8.0	6.7	
Thimena	Thimena	20/1/21	13:15	26.454445	37.58275	147	-7.5	6.5	
Samos	Gaggos beach	11/1/21	8:08	26.964569	37.76557	31	-9.1	7.4	
Samos	Ag. Paraskevi	11/1/21	10:01	26.993232	37.78102	31	-9.1	7.4	
Samos	Asprochorti	5/2/21	13:41	26.981603	37.78284	31	-9.1	7.4	
Samos	Livadaki	5/2/21	12:29	26.984829	37.79435	31	-9.1	7.4	

Table 1 (continued)

WL measurements							Tidal model		
Island	Location	Date	Time (UTC)	Lon (deg)	Lat (deg)		Nearest cell depth (m)	Min. amp. (cm)	Max amp (cm)
Samos	Charavgi	5/2/21	15:35	27.035123	37.73		30	-7.8	7.3
Samos	Kokkari	11/1/21	13:08	26.89314	37.78028		74	-9.1	7.5
Samos	Avlakia	11/1/21	13:41	26.857284	37.7986		111	-9.1	7.5
Samos	Ag. Konstantinos	11/1/21	14:12	26.816526	37.80816		129	-9.1	7.5
Samos	Ag. Nikolaos	11/1/21	15:33	26.742111	37.81287		80	-9.1	7.6
Samos	Karlovasi	13/1/21	7:25	26.678726	37.79614		235	-9.1	7.6
Samos	Marathokampos	13/1/21	9:25	26.699904	37.70981		86	-8.6	7.5
Samos	Ireo	13/1/21	10:59	26.883216	37.66014		45	-7.8	7.3
Samos	Pythagorion	31/10/20	8:35	26.94289	37.68866		26	-7.8	7.3
Samos	Malagari	11/1/21	11:01	26.960658	37.75115		31	-9.1	7.4
Samos	Vathi	4/2/21	12:15	26.975827	37.75581		31	-9.1	7.4

Table 2 Tsunami field measurements collected in the Greek islands. Date types: TE = Tsunami Elevation, EM = Elevation Measurement of a coastal feature that was flooded by the tsunami, RU = (vertical) runup, IN = (horizontal) inundation distance, DD = (vertical) drawdown, FD = (vertical) flow depth. See Fig. 2 for visual description of parameters

Point ID	Lat (deg)	Lon (deg)	Data type	Value (m)	Location	Notes
<i>Chios</i>						
C1-1	38.188008	26.028245	TE	1.38	Emporios	Stairs leading to taverna “Porto Emborios” where the maximum water level reached according to the owner
C1-2	38.188183	26.027884	IN	70	Emporios	Inundation point
C2	38.202046	26.049063	RU	1.44	Komi	Runup point just inland of Komi harbour. Indicated by an eyewitness
C2	38.202046	26.049063	IN	12	Komi	Inundation for the same point
C3	38.241741	26.106489	TE	0.82	Vokaria	Maximum tsunami elevation point measured at the side of the harbour dock. Indicated by a local resident
C4	38.265574	26.103296	TE	0.75	Katarraktis	Maximum tsunami elevation point measured at the top of the harbour dock. Indicated by eyewitnesses. FD = 5 cm from dock level
C5	38.283665	26.11824	RU	0.65	Ag. Ioannis	Runup point measured at the slip of the harbour. Indicated by eyewitness and confirmed through eyewitness pictures
C6	38.357033	26.14352	TE	0.52	Farkena	Maximum tsunami elevation point indicated by an eyewitness on an armour rock inside the harbour basin. Confirmed by another fisherman/eyewitness
C7	38.372222	26.137751	TE	0.32	Chios Port	Elevation of a rubber tire/fender hanging on the side of the dock. Indicated by the owner of the kiosk next to the customs building
<i>Ikarria</i>						
I1	37.632272	26.102797	RU	0.92	Gialiskari	A local resident indicated the maximum wave runup point reached along the harbour slip during the first and largest wave. Not an eyewitness, relayed information from others
I1	37.632272	26.102797	IN	6	Gialiskari	Inundation for the same point
I2	37.631363	26.180027	EM	1.18	Evdilos	Elevation of dock running along the perimeter of the harbour that appears flooded in CCTV video
I3	37.63415	26.216981	RU	0.97	Karavostamo	Runup point on a broken wall corner. Indicated by a local resident who was relaying the account of eyewitnesses
I3	37.63415	26.216981	IN	25.8	Karavostamo	Inundation for the same point
I4	37.686107	26.343209	RU	0.91	Ag. Kiriaki	Runup point on the harbour slip. Indicated by an eyewitness
I4	37.686107	26.343209	IN	6.5	Ag. Kiriaki	Inundation for the same point

Table 2 (continued)

Point ID	Lat (deg)	Lon (deg)	Data type	Value (m)	Location	Notes
I5	37.673002	26.351707	EM	0.79	Fanari	Elevation of the dock that locals indicated was covered with water
I6	37.622663	26.305387	EM	0.79	Therna	Elevation of dock an eyewitness indicated was covered with water
I7-1	37.616014	26.298375	TE	0.82	Ag. Kirikos-marina	Elevation of rubber/fender running along the side of the dock that the maximum water level reached in the marina according to eyewitnesses
I7-2	37.614348	26.295276	EM	0.86	Ag. Kirikos	Elevation of the higher of the two docks that appear to be flooded in CCTV video
I8	37.556635	26.117919	RU	0.51	Magganitis	Runup corresponding to a sitting area in the harbour that was flooded according to a local resident
I8	37.556635	26.117919	IN	6.2	Magganitis	Inundation for the same point
<i>Fourni</i>						
F1-1	37.576892	26.479918	TE	1.31	Fourni	Tsunami elevation point indicated by the carpenter whose business is next to the point
F1-2	37.577329	26.480019	RU	1.28	Fourni	Runup point according to eyewitness
F1-2	37.577329	26.480019	IN	24.6	Fourni	Inundation for the same point
F1-3	37.577801	26.480088	TE	1.44	Fourni	Tsunami elevation point at the last step to the entrance of Antica Chocolateria Bakery according to the owner. FD = 20 cm from pavement, FD = 33 cm from street level
F1-4	37.577708	26.480145	TE	1.42	Fourni	Tsunami elevation point inside Proton Supermarket. FD = 20 cm from street level
F1-5	37.577673	26.480318	RU	1.57	Fourni	Runup point indicated by eyewitnesses
F1-5	37.577673	26.480318	IN	49.1	Fourni	Inundation for the same point
F2	37.591709	26.505587	EM	0.96	Bali	Highest elevation point of the harbour dock which was covered with water according to eyewitnesses
F3	37.628163	26.506743	RU	1.18	Chrisomillia	Runup point according to a local fisherman
F3	37.628163	26.506743	IN	19	Chrisomillia	Inundation for the same point
F4	37.598882	26.532921	RU	1.25	Kamari	Approximate runup point according to the owner of taverna “Almyra”
F4	37.598882	26.532921	IN	20.7	Kamari	Inundation for the same point
<i>Thimena</i>						
T1	37.582458	26.453472	TE	1.46	Thimena	Elevation of the first step at the end of the harbour dock where the maximum water elevation reached according to eyewitnesses. FD = 23 cm from dock level

Table 2 (continued)

Point ID	Lat (deg)	Lon (deg)	Data type	Value (m)	Location	Notes
<i>Samos</i>						
S1-1	37.795116	26.67828	RU	2.08	Karlovasi	Runup point in the boat maintenance area. Indicated by eyewitness and confirmed through pictures
S1-1	37.795116	26.67828	IN	55.7	Karlovasi	Inundation for the same point
S1-2	37.796084	26.678651	DD	-1.21	Karlovasi	Drawdown point identified through an eyewitness photo taken on 30 October 2020 at 11:55 UTC
S1-3	37.794502	26.680252	RU	1.88	Karlovasi	Runup point in front of a house. Indicated by eyewitness
S1-3	37.794502	26.680252	IN	55.3	Karlovasi	Inundation for the same point
S1-4	37.794214	26.682689	RU	1.96	Karlovasi	Runup point next to Relax Café Patisserie. Indicated by eyewitness
S1-4	37.794214	26.682689	IN	36.1	Karlovasi	Inundation for the same point
S1-5	37.796464	26.687001	TE	0.99	Karlovasi	Tsunami elevation identified on the side of a temporary structure. FD = 5 cm from ground
S1-6	37.794915	26.686501	RU	1.85	Karlovasi	Runup point indicated by eyewitness
S1-6	37.794915	26.686501	IN	82.5	Karlovasi	Inundation for the same point
S2	37.81271	26.742123	TE	2.98	Ag. Nikolaos	Elevation of the lower part of the "Beach" sign on the wall (splash on wall, see text for details)
S3	37.808316	26.816561	TE	0.63	Ag. Konstantinos	Elevation of a step on harbour dock reached by the maximum water level. Indicated by an eyewitness
S4-1	37.799189	26.857104	RU	0.62	Avlakia	Runup point on concrete terrace in front of a waterfront house. Indicated by an eyewitness
S4-1	37.799189	26.857104	IN	6.8	Avlakia	Inundation for the same point
S4-2	37.798596	26.857285	DD	-0.95	Avlakia	Drawdown point. An eyewitness described the shoreline receding to that point
S5	37.780309	26.893043	RU	0.73	Kokkari	Runup point on the beach inside the harbour. Indicated by an eyewitness
S5	37.780309	26.893043	IN	9.2	Kokkari	Inundation for the same point
S6-1	37.757543	26.955781	RU	1.03	Malagari	Runup point indicated by an eyewitness (owner of Moto Service Karydas)
S6-1	37.757543	26.955781	IN	52	Malagari	Inundation for the same point
S6-2	37.755518	26.957241	RU	0.97	Malagari	Runup point in the parking lot of Roussakis Marine. Indicated by the owner of the business
S6-2	37.755518	26.957241	IN	53.8	Malagari	Inundation for the same point

Table 2 (continued)

Point ID	Lat (deg)	Lon (deg)	Data type	Value (m)	Location	Notes
S6-3	37.75548	26.956987	TE	0.98	Malagari	Tsunami elevation point on top of a step leading to the entrance to a waterfront house. Indicated by an eyewitness
S6-4	37.750989	26.96035	RU	1.38	Malagari	Runup point on the ramp of the Nioti service store. Indicated by the owner/eyewitness
S6-4	37.750989	26.96035	IN	32.7	Malagari	Inundation for the same point
S7-1	37.7525401	26.9770241	TE	1.21	Vathi	Plaisir coffees store. FD = 23 cm from street level
S7-2	37.7528257	26.9771992	TE	0.94	Vathi	Inside Frazzeskos Distillery store. FD = 22 cm from store floor
S7-3	37.7532461	26.9771469	TE	1.13	Vathi	Outside store “My Style”. FD = 39 cm from pavement level
S7-4	37.7535529	26.9772458	TE	1.58	Vathi	Entrance to “Coffee Lab”
S7-5	37.7536998	26.9771996	TE	1.45	Vathi	Entrance to the “Carousel” store
S7-6	37.7538739	26.9772546	TE	1.18	Vathi	Inside Tsoumakis nautical supplies. FD = 5 cm from store floor
S7-7	37.7541302	26.9776837	IN	82.6	Vathi	Approximate inundation point. Indicated by eyewitnesses
S7-8	37.754148	26.9775439	TE	1.20	Vathi	Kiosk. FD = 27 cm from street level
S7-9	37.7544543	26.977239	TE	1.28	Vathi	Bazaar Super Market. FD = 5 cm from store floor
S7-10	37.7545137	26.9771595	TE	1.25	Vathi	Hondos Center entrance. FD = 70 cm from pavement level
S7-11	37.7550268	26.9770151	TE	1.42	Vathi	Bank of Greece steps. FD = 100 cm from street level
S7-12	37.7550948	26.9772321	TE	1.43	Vathi	In front of a dusty store window along the lane next to the Bank of Greece branch. FD = 95 cm from street level
S7-13	37.755102	26.9773637	TE	1.33	Vathi	Water level inside Nova store. FD = 70 cm from street level
S7-14	37.755099	26.9776471	TE	1.31	Vathi	Water level inside di Mario shoe store. FD = 12 cm from store floor
S7-15	37.755665	26.977428	RU	1.77	Vathi	Runup point along Cpt. Stamatidis street
S7-15	37.755665	26.977428	IN	106	Vathi	Inundation for the same point
S7-16	37.7557168	26.9772957	RU	1.59	Vathi	Runup point along Kyrillou St
S7-16	37.7557168	26.9772957	IN	98	Vathi	Inundation for the same point
S7-17	37.7562014	26.9768673	RU	1.98	Vathi	Runup point along Ag. Nikolaou St
S7-17	37.7562014	26.9768673	IN	96	Vathi	Inundation for the same point
S7-18	37.7563249	26.9767113	TE	1.72	Vathi	Blue Roots Nuts Grocery Store. FD = 22 cm from street level

Table 2 (continued)

Point ID	Lat (deg)	Lon (deg)	Data type	Value (m)	Location	Notes
S7-19	37.7566549	26.9763639	TE	1.85	Vathi	Kanakakis Store. FD = 25 cm from store floor
S7-20	37.7568643	26.975981	RU	1.91	Vathi	Runup point in Ag. Nikolaos square
S7-20	37.7568643	26.975981	IN	108	Vathi	Inundation for the same point
S7-21	37.756147	26.9762263	TE	1.66	Vathi	Armodios Bakery. FD = 88 cm from store floor
S7-22	37.7564297	26.9763809	TE	1.74	Vathi	Grigoris store. FD = 70 cm from pavement level
S7-23	37.7563686	26.9759205	TE	1.85	Vathi	Charas souvenir store. FD = 100 cm from pavement level, FD = 115 cm from street level
S7-24	37.756923	26.9747185	TE	1.18	Vathi	Pharmacy. FD = 60 cm from pavement/street level
S7-25	37.7570339	26.9747659	TE	1.31	Vathi	No name store. FD = 47 cm from pavement/street level
S7-26	37.757196	26.9749224	TE	1.56	Vathi	Close to runup/inundation point. FD = 20 cm from pavement/street level
S7-27	37.7570485	26.9739481	TE	1.36	Vathi	Inside the mini-market. FD = 64 cm from store floor
S7-28	37.7577578	26.9737091	RU	1.78	Vathi	Runup point right next to an eyewitness' house
S7-28	37.7577578	26.9737091	IN	94	Vathi	Inundation for the same point
S7-29	37.7575183	26.9728453	TE	1.52	Vathi	Entrance of AutoUnion Car rental store. FD = 80 cm from pavement
S7-30	37.7576834	26.9728608	TE	1.59	Vathi	Along Grammou St. FD = 27 cm from street level
S7-31	37.7576158	26.9723026	EM	1.38	Vathi	Elevation of tabletop in front of Rhenia tours which the maximum water level exceeded. Vertical distance to pavement = 77 cm
S7-32	37.7577062	26.9722637	TE	1.54	Vathi	Inside Pizzeria Appaloussa. FD = 72 cm from store floor
S7-33	37.757806	26.971348	RU	1.92	Vathi	Runup point on stairs in front of the travel office. Indicated by an eyewitness
S7-33	37.757806	26.971348	IN	22.5	Vathi	Inundation for the same point
S8	37.765361	26.964955	RU	0.91	Gaggos beach	Wreck line identified on beach
S8	37.765361	26.964955	IN	7.6	Gaggos beach	Inundation for the same point
S9-1	37.779263	26.982792	RU	1.74	Asprochorti	Runup point along the road leading to the house of the eyewitness
S9-1	37.779263	26.982792	IN	40	Asprochorti	Inundation for the same point
S9-2	37.782954	26.981743	RU	1.44	Asprochorti	Runup point in a small beach north of Asprochorti according to an eyewitness in Asprochorti
S9-2	37.782954	26.981743	IN	17.5	Asprochorti	Inundation for the same point

Table 2 (continued)

Point ID	Lat (deg)	Lon (deg)	Data type	Value (m)	Location	Notes
S10	37.79462	26.985316	RU	0.68	Livadaki	Runup point according to the owner of the business/eyewitness
S10	37.79462	26.985316	IN	52.5	Livadaki	Inundation for the same point
S11	37.781006	26.993245	TE	0.59	Ag. Paraskevi	Tsunami elevation point on steps next to the dock. Indicated by an eyewitness
S12	37.7296	27.035314	TE	0.34	Charvagi	Tsunami elevation point on a wooden jetty. Indicated by an eyewitness
S13-1	37.690099	26.943089	DD	-0.43	Pythagorion	A drawdown point on the side of the dock according to an eyewitness
S13-2	37.690104	26.943093	TE	0.61	Pythagorion	A tsunami elevation point on the side of the dock according to an eyewitness
S13-3	37.688673	26.942874	TE	0.53	Pythagorion	The water just made it to the top of the harbour dock according to an eyewitness
S14	37.660126	26.883229	TE	0.53	Ireo	Tsunami elevation point measured at the steps of the harbour dock. Indicated by eyewitnesses
S15	37.709847	26.699884	RU	0.63	Marathokampos	Runup point on the beach inside the harbour. Indicated by an eyewitness and confirmed through eyewitness pictures. Beach morphology might have changed since the earthquake—use as a proxy
S15	37.709847	26.699884	IN	4.3	Marathokampos	Inundation for the same point

Acknowledgements NK and NM acknowledge financial support by the project “HELPOS-HELlenic Plate Observing System” (MIS5002697), implemented under the Action “Reinforcement of the Research and Innovation Infrastructure”, funded by the Operational Programme “Competitiveness, Entrepreneurship and Innovation” (NSRF 2014-2020) and co-financed by Greece and the European Union (European Regional Development Fund). The authors would like to acknowledge Mr. Vorias (local civil protection office in Chios), Mr. Koutras (police office in Samos) and Mr. Tsaparikos (port police office in Samos) for the valuable information they provided over the phone interviews regarding the timing, response and impact of the tsunami in Chios and Samos. The authors would like to thank the Municipality and the Mayor of E. Samos, Mr. Stantzos, for their warm welcome and their support for our work. The authors warmly thank the Hellenic Coast Guard and the crew of the boat that transported team members to Fourni and Thimena. Last but not least, the authors acknowledge all eyewitnesses who provided us with their valuable accounts of the events on October 30th, 2020 and for sharing with us pictures and videos of the tsunami that helped us better understand the timing of impact in the various locations visited in the post-tsunami reconnaissance missions. Figures were built using the Generic Mapping Tools (Wessel et al. 2013).

Funding The travel costs of NK, VS and NM in the post-tsunami reconnaissance missions (besides the first trip the day after the earthquake) were funded by the Joint Research Centre of the European Commission (Tender No. JRC/IPR/2020/VLVP/2898).

Availability of data and materials The data points are made available in the Appendix. The tsunami hydrograph and overland flow velocity data inferred through the analysis of the Samos Library CCTV videos can be shared upon reasonable request.

Code availability Not applicable.

Declarations

Conflict of interest The authors declare that they have no known competing financial interests or personal relationships that could have appeared to influence the work reported in this paper.

References




- Aksoy ME (2021) Post-event field observations in the İzmir-Sığacık village for the tsunami of the 30 October 2020 Samos (Greece) M_w 6.9 earthquake. *Acta Geophys* 69:1113–1125. <https://doi.org/10.1007/s11600-021-00582-w>
- Ambraseys N, Synolakis C (2010) Tsunami catalogs for the Eastern Mediterranean, revisited. *J Earthquake Eng* 14(3):309–330. <https://doi.org/10.1080/13632460903277593>
- Andrew J, Cooper G (2005) Microtidal coasts. In: *Encyclopedia of coastal science*. Ed: Schwartz ML, Springer Netherlands, Dordrecht, pp 638–638
- Astraparis (2020) The boats on the rocks in Komi - damage in Chalkeos. *Astraparis Chios News Online*. URL <https://astraparis.gr/sta-vrachia-oi-varkes-stin-komi-zimies-sto-chalkeios/>. Date published: 30–10–2020, Accessed: 05–11–2020.
- Bird P (2003) An updated digital model of plate boundaries. *Geochem Geophys Geosyst* 4(3):1027. <https://doi.org/10.1029/2001GC000252>
- Borrero JC, Lynett PJ, Kalligeris N (2015) Tsunami currents in ports. *Proc R Soc Lond A* 373:20140372. <https://doi.org/10.1098/rsta.2014.0372>
- Chatzipetros A, Kiratzi A, Sboras S, Zouros N, Pavlides S (2013) Active faulting in the north-eastern Aegean Sea Islands. *Tectonophysics* 597–598:106–122. <https://doi.org/10.1016/j.tecto.2012.11.026>
- Cirella A, Romano F, Avallone A, Piatanesi A, Briole P, Ganas A, Theodoulidis N, Chousianitis K, Volpe M, Bozionellos G, Selvaggi G (2020) The 2018 M_w 6.8 Zakynthos (Ionian Sea, Greece) earthquake: Seismic source and local tsunami characterization. *Geophys J Int* 221(2):1043–1054. <https://doi.org/10.1093/gji/ggaa053>
- Dogan GG, Annunziato A, Papadopoulos GA, Guler HG, Yalciner AC, Cakir TE, Sozdinler CO, Ulutas E, Arikawa T, Suzen ML, Guler I (2019) The 20th July 2017 Bodrum-Kos Tsunami Field Survey. *Pure Appl Geophys* 176(7):2925–2949. <https://doi.org/10.1007/s00024-019-02151-1>
- Dogan GG, Yalciner AC, Yuksel Y, Ulutaş E, Polat O, Güler I, Şahin C, Tarih A, Kânoğlu U (2021) The 30 October 2020 Aegean Sea tsunami: post-event field survey along Turkish coast. *Pure Appl Geophys* 178(3):785–812. <https://doi.org/10.1007/s00024-021-02693-3>

- Dogan GG, Kalligeris N, Yalciner AC, Charalampakis M, et al. (2020) Tsunami effects and performance of port structures (chapter 2). In: Seismological and Engineering Effects of the M 7.0 Samos Island (Aegean Sea) Earthquake, Ed: Onder Çetin K, Mylonakis G, Sextos A, Stewart JP, Geotechnical Extreme events reconnaissance association: Report GEER-069.
- Dominey-Howes D, Dengler L, Dunbar P, Kong L, Fritz H, Imamura F, Borrero J (2014) International tsunami survey team (ITST) post-tsunami survey field guide. UNESCO-IOC, Paris, p 475
- Egbert GD, Erofeeva SY (2002) Efficient inverse modeling of barotropic ocean tides. *J Atmos Oceanic Tech* 19(2):183–204. [https://doi.org/10.1175/1520-0426\(2002\)019%3c0183:EIMOBO%3e2.0.CO;2](https://doi.org/10.1175/1520-0426(2002)019%3c0183:EIMOBO%3e2.0.CO;2)
- England P, Howell A, Jackson J, Synolakis C (2015) Palaeotsunamis and tsunami hazards in the Eastern Mediterranean. *Proc R Soc Lond A* 373(2053):20140374. <https://doi.org/10.1098/rsta.2014.0374>
- Erdik M, Demircioğlu MB, Cüneyt T (2020) Forensic analysis reveals the causes of building damage in İzmir in the Oct. 30 Aegean Sea earthquake. *Tembler*, <https://doi.org/10.32858/temblor.139>.
- Esteban M, Thao ND, Takagi H, Tsimopoulou V, Mikami T, Yun NY, Suppasri A (2015) The emergence of global tsunami awareness: Analysis of disaster preparedness in Chile, Indonesia, Japan, and Vietnam. In *Handbook of coastal disaster mitigation for engineers and planners*, Ed: Esteban M, Takagi H, Shibayama T. Butterworth-Heinemann, <https://doi.org/10.1016/B978-0-12-801060-0.00011-3>.
- Fritz HM, Kalligeris N (2008) Ancestral heritage saves tribes during 1 April 2007 Solomon Islands tsunami. *Geophys Res Lett* 35(1):L01607. <https://doi.org/10.1029/2007GL031654>
- Fritz HM, Borrero JC, Synolakis CE, Yoo J (2006) 2004 Indian Ocean tsunami flow velocity measurements from survivor videos. *Geophys Res Lett* 33:L24605. <https://doi.org/10.1029/2006GL026784>
- Fritz HM, Phillips DA, Okayasu A, Shimozone T, Liu H, Mohammed F, Skanavis V, Synolakis CE, Takahashi T (2012) The 2011 Japan tsunami current velocity measurements from survivor videos at Kesennu Bay using LiDAR. *Geophysical Research Letters*, 39:L00G23, <https://doi.org/10.1029/2011GL050686>.
- Fritz HM, Synolakis C, Kalligeris N, Skanavis V, Santoso F, Rizal M, Prasetya GS, Liu Y, Liu PL (2018) Field survey of the 28 September 2018 Sulawesi tsunami. In *AGU Fall Meeting Abstracts (Vol. 2018, pp. NH22B-04)*.
- Ganas A, Briole P, Bozionelos G, Barberopoulou A, Elias P, Tsironi V, Valkaniotis S, Moshou A, Mintourakis I (2020) The 25 October 2018 Mw = 6.7 Zakynthos earthquake (Ionian Sea, Greece): A low-angle fault model based on GNSS data, relocated seismicity, small tsunami and implications for the seismic hazard in the west Hellenic Arc. *J Geodyn* 137:101731. <https://doi.org/10.1016/j.jog.2020.101731>
- Ganas A, Elias P, Briole P, Valkaniotis S, Escartin J, Tsironi V, Karasante I, Kosma C (2021) Co-seismic and post-seismic deformation, field observations and fault model of the 30 October 2020 $M_w = 7.0$ Samos earthquake Aegean Sea. *Acta Geophys* 69:999–1024. <https://doi.org/10.1007/s11600-021-00599-1>
- GEBCO (2020) GEBCO Bathymetry portal. URL <http://www.gebco.net>, Accessed: 12–12–2020.
- Heidarzadeh M, Gusman AR (2021) Source modeling and spectral analysis of the Crete tsunami of 2nd May 2020 along the Hellenic Subduction Zone, offshore Greece. *Earth, Planets Space* 73(1):1–16. <https://doi.org/10.1186/s40623-021-01394-4>
- Heidarzadeh M, Necmioğlu O, Ishibe T, Yalciner AC (2017) Bodrum-Kos (Turkey–Greece) Mw 6.6 earthquake and tsunamis of 20 July 2017: a test for the Mediterranean tsunami warning system. *Geosci Lett* 4(1):1–11. <https://doi.org/10.1186/s40562-017-0097-0>
- Holland KT, Holman RA, Lippmann TC, Stanley J, Plant N (1997) Practical use of video imagery in nearshore oceanographic field studies. *IEEE J Oceanic Eng* 22(1):81–92. <https://doi.org/10.1109/48.557542>
- Kalligeris N, Skanavis V, Tavakkol S, Ayca A, Safty HE, Lynett P, Synolakis C (2016) Lagrangian flow measurements and observations of the 2015 Chilean tsunami in Ventura CA. *Geophys Res Lett* 43:5217–5224. <https://doi.org/10.1002/2016GL068796>
- Kalligeris N, Kim Y, Lynett PJ (2021) Wave-induced shallow-water monopolar vortex: large-scale experiments. *J Fluid Mech* 910:A17. <https://doi.org/10.1017/jfm.2020.980>
- Kiratzis A, Ozacar AA, Papazachos C, Pınar A, et al. (2020) Regional Tectonics and Seismic Source (Chapter 1). In: *Seismological and engineering effects of the M 7.0 Samos Island (Aegean Sea) Earthquake*, Ed: Onder Çetin K, Mylonakis G, Sextos A, Stewart JP, Geotechnical extreme events reconnaissance association: Report GEER-069.
- Lentas K, Gkarlaoui C, Kalligeris N, Melis NS (2021) The 30 October 2020, Mw 7.0, Samos earthquake: aftershock relocation, slip model, Coulomb stress evolution and estimation of shaking. *Bull Earthq Eng*. <https://doi.org/10.1007/s10518-021-01260-4>
- Melis NS, Okal EA, Synolakis CE, Kalogeras IS, Kânoğlu U (2020) The chios greece earthquake of 23 July 1949: seismological reassessment and tsunami investigations. *Pure Appl Geophys* 177(3):1295–1313. <https://doi.org/10.1007/s00024-019-02410-1>

- Meng J, Sinoplu O, Zhou Z, Tokay B, Kusky T, Bozkurt E, Wang L (2021) Greece and Turkey Shaken by African tectonic retreat. *Sci Rep* 11:6486. <https://doi.org/10.1038/s41598-021-86063-y>
- Nomikou P, Evangelidis D, Papanikolaou D, Lampridou D, Litsas D, Tsaparas Y, Koliopoulos I (2021) Morphotectonic analysis along the northern margin of Samos Island, related to the seismic activity of October 2020, Aegean Sea Greece. *Geosciences* 11(2):102. <https://doi.org/10.3390/geosciences11020102>
- Okal EA, Synolakis CE (2004) Source discriminants for near-field tsunamis. *Geophys J Int* 158(3):899–912. <https://doi.org/10.1111/j.1365-246X.2004.02347.x>
- Okal EA, Synolakis CE, Uslu B, Kalligeris N, Voukouvalas E (2009) The 1956 earthquake and tsunami in Amorgos Greece. *Geophys J Int* 178(3):1533–1554. <https://doi.org/10.1111/j.1365-246X.2009.04237.x>
- Styron R, Pagani M (2020) The GEM global active faults database. *Earthq Spectra* 36:160–180. <https://doi.org/10.1177/8755293020944182>
- Swaminathan R, Nayar SK (2002) Nonmetric calibration of wide-angle lenses and polycameras. *IEEE Trans Pattern Anal Mach Intell* 22(10):1172–1178. <https://doi.org/10.1109/34.879797>
- Synolakis C, Okal E (2005) 1992–2002: Perspective on a decade of post-tsunami surveys. In: Satake K. (eds) *Tsunamis. Advances in natural and technological hazards research*, https://doi.org/10.1007/1-4020-3331-1_1.
- Tadepalli S, Synolakis CE (1994) The run-up of N-waves on sloping beaches. *Proc R Soc Lond A* 445:99–112. <https://doi.org/10.1098/rspa.1994.0050>
- Triantafyllou I, Gogou M, Mavroulis S, Lekkas E, Papadopoulos GA, Thravalos M (2021) The Tsunami Caused by the 30 October 2020 Samos (Aegean Sea) Mw7.0 Earthquake: Hydrodynamic features, source properties and impact assessment from post-event field survey and video records. *J Marine Sci Eng* 9(1):68. <https://doi.org/10.3390/jmse9010068>
- Tuncag M, Lekkas E, Mavroulis S, et al. (2020) Emergency response and societal impact/recovery (Chapter 8). In: *Seismological and engineering effects of the M 7.0 Samos Island (Aegean Sea) Earthquake*, Ed: Onder Çetin K, Mylonakis G, Sextos A, Stewart JP, geotechnical extreme events reconnaissance association: Report GEER-069
- Tur H, Yaltrak C, Elitez İ, Sarıkavak KT (2015) Pliocene-Quaternary tectonic evolution of the Gulf of Gökova, southwest Turkey. *Tectonophysics* 638:158–176. <https://doi.org/10.1016/j.tecto.2014.11.008>
- UNESCO (2014) International Tsunami Survey Team (ITST) Post-Tsunami Survey Field Guide. 2nd Edition, Ed: Dominey-Howes D and Dengler L, IOC Manuals and Guides No. 37, Paris: UNESCO (English).
- URANUS (2021) The URANUS reference station network (in Greek). URL <http://www.uranus.gr>. Accessed: 21–04–2021.
- Wessel P, Smith WHF, Scharroo R, Luis J, Wobbe F (2013) Generic mapping tools: Improved version released. *EOS Trans Am Geophys Union* 94(45):409–410. <https://doi.org/10.1002/2013eo450001>
- YouTube (2020a) Tsunami in Ag. Kirikos, Ikaría on 30/10/2020 (in Greek). URL <https://youtu.be/LC4KMlNbuag>. Date published: 09–11–2020, Accessed: 21–04–2021.
- YouTube (2020b) Tsunami in Evdilos on 30/10/2020 (in Greek). URL <https://youtu.be/F10EgzaD9s8> Date published: 05–11–2020, Accessed: 21–04–2021.
- YouTube (2020c) Unbelievable - Tsunami after the earthquake in Samos (in Greek). URL https://youtu.be/_ef3NfEJKQ. Date published: 15–11–2020, Accessed: 21–04–2021.

Publisher's Note Springer Nature remains neutral with regard to jurisdictional claims in published maps and institutional affiliations.

Authors and Affiliations

Nikos Kalligeris¹  · **Vassilios Skanavis**²  · **Marinos Charalampakis**¹  ·
Nikolaos S. Melis¹ · **Evangelos Voukouvalas**³  · **Alessandro Annunziato**⁴ ·
Costas E. Synolakis²

Vassilios Skanavis
skanavis@usc.edu

Marinos Charalampakis
cmarinos@noa.gr

Nikolaos S. Melis
nmelis@noa.gr

Evangelos Voukouvalas
vvoukouvalas@gmail.com

Alessandro Annunziato
alessandro.annunziato@ec.europa.eu

Costas E. Synolakis
costas@usc.edu

¹ Institute of Geodynamics, National Observatory of Athens, Athens, Greece

² Academy of Athens, Athens, Greece

³ Unisystems Luxembourg Sarl, Bertrange, Luxembourg

⁴ Joint Research Centre, European Commission, Ispra, Italy